

See discussions, stats, and author profiles for this publication at: <https://www.researchgate.net/publication/270344470>

# Pharmacophore modeling, drug design and virtual screening on multi-targeting procognitive agents approaching histaminergic pathways

ARTICLE *in* JOURNAL OF THE TAIWAN INSTITUTE OF CHEMICAL ENGINEERS · JANUARY 2015

Impact Factor: 3 · DOI: 10.1016/j.jtice.2014.09.017

---

READS

82

## 3 AUTHORS:



**Katarina Nikolic**

University of Belgrade

61 PUBLICATIONS 236 CITATIONS

SEE PROFILE



**Agbaba Danica**

University of Belgrade

131 PUBLICATIONS 931 CITATIONS

SEE PROFILE

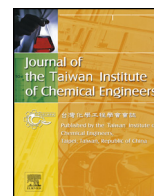


**Holger Stark**

Heinrich-Heine-Universität Düsseldorf

377 PUBLICATIONS 5,724 CITATIONS

SEE PROFILE



# Pharmacophore modeling, drug design and virtual screening on multi-targeting procognitive agents approaching histaminergic pathways

Katarina Nikolic<sup>a,\*</sup>, Danica Agbaba<sup>a</sup>, Holger Stark<sup>b</sup>

<sup>a</sup> University of Belgrade, Faculty of Pharmacy, Department of Pharmaceutical Chemistry, Vojvode Stepe 450, 11000 Belgrade, Serbia

<sup>b</sup> Heinrich Heine University, Institute of Pharmaceutical and Medicinal Chemistry, Universitaetsstr. 1, 40225 Duesseldorf, Germany

## ARTICLE INFO

### Article history:

Received 27 March 2014

Received in revised form 8 August 2014

Accepted 21 September 2014

Available online 16 October 2014

### Keywords:

Drug design

3D-QSAR

Histamine H<sub>3</sub> receptor

Histamine N-methyltransferase

Pharmacophore

Virtual screening

## ABSTRACT

In an effort to design dual acting compounds enhancing histaminergic neurotransmission in the central nervous system, a novel class of 35 non-imidazole histamine H<sub>3</sub> receptor (H<sub>3</sub>R) antagonists that simultaneously possess strong inhibitory potency on catabolic histamine N-methyltransferase (HMT), have been examined by 3D-QSAR study.

For improved understanding, the crucial chemical functionalities for combined H<sub>3</sub>R/HMT activities 3D-QSAR pharmacophore models (H<sub>3</sub>R:  $R^2$  (0.98),  $Q^2$  (0.94), RMSE (0.171); and HMT:  $R^2$  (0.80),  $Q^2$  (0.60), RMSE (0.159) were developed.

Pharmacophore for H<sub>3</sub>R antagonistic activity mainly differs from pharmacophore for HMT inhibiting activity in presence of specific lipophilic/steric components of the H<sub>3</sub>R pharmacophore, H-bond accepting components of the H<sub>3</sub>R pharmacophore, H-bond donating components of the HMT pharmacophore, and longer optimal distance between H-bond donor and steric hot spots in the H<sub>3</sub>R pharmacophore than in the HMT pharmacophore.

Formed 3D-QSAR models were applied for design of novel piperidino-aminoquinoline hybrids as multitarget H<sub>3</sub>R/HMT ligands with potential impact in therapy of sleep-wake disorders and cognitive impairment. Designed compounds with 3D-QSAR predicted  $pK_i$  (H<sub>3</sub>R) > 9.6 and ( $pK_i$  (H<sub>3</sub>R) +  $pIC_{50}$ (HMT)) > 16.8 were selected for further profiling.

Virtual screening of ZINC database is performed against the most promising H<sub>3</sub>R/HMT ligand and top ranked compounds are tested by both 3D-QSAR models.

© 2014 Taiwan Institute of Chemical Engineers. Published by Elsevier B.V. All rights reserved.

## 1. Introduction

Histamine is a well-known chemical mediator in the immediate allergic response, regulation of gastric acid secretion, and also plays a role as a neurotransmitter in the central nervous system (CNS) [1]. In the CNS neurons, histamine is synthesized from L-histidine by cytoplasmatic L-histidine decarboxylase enzyme (HDC, E.C. 4.1.1.22) and then stored in the vesicles and released from the axon terminals in a calcium-dependent rapid-turnover mechanism [1,2]. The main inactivation procedure in the CNS is an enzymatic catabolic process occurring in the nearest glia cells [2]. In the brain histamine is mainly inactivated by methylation of the imidazole ring in the N<sup>t</sup>-position, catalyzed by histamine N-methyltransferase enzyme (HMT, E.C. 2.1.1.8) [2,3]. Histamine

mediated its main biological activities by interaction with four distinct histamine receptors (H<sub>1</sub>R–H<sub>4</sub>R, which are members of the class A family of G-protein coupled receptors (GPCRs) [1,3]. Pharmacological studies of frontocortical histaminergic pathways confirmed that antagonism of negative feed-back mechanism presynaptic histamine H<sub>3</sub> autoreceptors reinforces histaminergic transmission, while blockade of histamine H<sub>3</sub> heteroreceptors accelerates the corticolimbic liberation of different neurotransmitters like dopamine, acetylcholine, glutamate, norepinephrine, GABA, and serotonin [4–7].

Recent pharmacological studies and clinical trials demonstrated that H<sub>3</sub>R play an essential role in regulation of the sleep-wake cycle and cognition. H<sub>3</sub>R antagonists assumed to have therapeutic effectiveness in the treatment of a sleep disorders (narcolepsy), cognitive impairment, pain/itch, stroke, depression, attention deficit hyperactivity disorder (ADHD), schizophrenia, dementia and neurodegenerative disorders (e.g. Parkinson's disease, Alzheimer's disease) [8–18].

\* Corresponding author. Tel.: +381 11 3951 259; fax: +381 11 3974 349.  
E-mail address: [knikolic@pharmacy.bg.ac.rs](mailto:knikolic@pharmacy.bg.ac.rs) (K. Nikolic).

Multitarget ligands displaying dual H<sub>3</sub>R antagonist/histamine N-methyltransferase (HMT) inhibiting properties are able to greatly enhance histaminergic neurotransmission by simultaneously combining histamine-releasing properties (via H<sub>3</sub> auto-receptor blockade), release of other neurotransmitters by complex receptor cross talk, and reduced catabolic rate for inactivation (via HMT inhibition) [19–23]. This novel approach of hybrid compounds targeting both H<sub>3</sub>R and HMT could contribute to the elevation of intersynaptic histamine levels in the CNS and might have therapeutic applications in psychiatric and neurodegenerative diseases [10,19–23].

In contrast to the early work on H<sub>3</sub>R [24], almost all chemical series of current clinical interest are non-imidazoles [25]. Major potential disadvantages of the imidazole derivatives are poor brain penetration, CYP450 inhibition, drug–drug interactions, liver toxicity, extrapyramidal symptoms, and inhibition of adrenal steroid synthesis [26–30].

Recently developed set of 35 multipotent ligands [19,20] containing a piperidinoalkyl group, as a key structural feature for human H<sub>3</sub>R antagonism, connected by different spacer lengths to an aminoquinoline moiety, as pharmacophoric moiety for HMT inhibiting activity, have been studied. The new class of non-imidazole derivatives [19,20] exerted moderate ( $K_i(\text{H}_3\text{R}): 1\text{--}100\text{ nM}$ ) to very high ( $K_i(\text{H}_3\text{R}): 0.09\text{--}1.80\text{ nM}$ ) affinity at human H<sub>3</sub>R and simultaneously possess strong ( $\text{IC}_{50}: 20\text{--}100\text{ nM}$ ) inhibiting activity on the HMT enzyme.

Based on our previous work in the synthesis and biological evaluation of the multipotent H<sub>3</sub>R/HMT inhibitors [19,20] and other multiple targeting ligands we have applied 3D-QSAR approach for design of novel dual H<sub>3</sub>R antagonists and HMR inhibitors as potential procognitive agents which may have additional properties on other precognitive targets, such as acetylcholinesterase (AChE) and butyrylcholinesterase (BChE).

The main aims of the 3D-QSAR study were to define specific molecular determinants for H<sub>3</sub>R antagonism and HMT inhibition of the 35 piperidino-aminoquinoline hybrids, design novel H<sub>3</sub>R/HMT ligands, and use 3D-QSAR models for evaluation of H<sub>3</sub>R antagonistic and HMT inhibiting activities of the newly designed compounds.

## 2. Materials and methods

### 2.1. 3D-QSAR study

The antagonist binding at H<sub>3</sub>R ( $K_i$ ) and inhibitory potency on HMT ( $\text{IC}_{50}$ ) of 35 aminoquinoline derivatives were used for the 3D-QSAR study [19,20]. Negative decadic logarithm of determined  $K_i$  and  $\text{IC}_{50}$ , i.e. ( $\text{p}K_i (\log(1/K_i))$  and  $\text{pIC}_{50} (\log(1/\text{IC}_{50}))$ ) values were calculated and used for the QSAR modeling. The  $\text{p}K_a$  calculation and selection of dominant molecules/cations at physiological pH 7.4 for the 35 examined compounds was performed by the MarvinSketch 5.5.1.0 program [31]. Dominant forms at physiological pH were further used for geometry optimization and for the 3D-QSAR study. Geometry optimization for the aminoquinoline derivatives was performed by *ab initio* Hartree–Fock/3–21G (HF/3–21) method [32] included in the Gaussian 98 program [33]. The selected HF/3–21 method was proven as very good choice for geometry optimization of related imidazoline, pyridine, piperidine derivatives and aromatic compounds [34–38]. Suitability of the HF/3–21 method for geometry optimization of the aminoquinolines was tested by comparing experimental and HF/3–21 tacrine conformations. Histamine methyltransferase (Natural Variant I105) complexed with the acetylcholinesterase Inhibitor and Alzheimer's disease drug tacrine (PDB: 2AOW) was used to obtain tacrine conformation in the enzyme active site. The experimental tacrine conformation was then superimposed with tacrine conformation obtained by use

of the (HF/3–21) method. Results of the overlay study (RMS error: 0.065) confirmed very high structural similarities between experimental and HF/3–21 tacrine conformations (Supplement material). Since tacrine and all examined ligands are aminoquinoline derivatives was concluded that the HF/3–21 is suitable method for geometry optimization of the data set.

The 3D-QSAR studies of the aminoquinoline derivatives were performed by use of the Pentacle 1.0.6 program [39] and Schrödinger–Phase software included in Maestro 2011 program [40,41]. The Pentacle 1.0.6 program [39] is advanced software tool for obtaining alignment-independent 3D quantitative structure–activity relationships. The 3D-QSAR starts from computing highly relevant 3D maps of interaction energies (GRID based Molecular Interaction Fields–MIFs) between the examined molecule and four chemical probes: DRY (which represent hydrophobic interactions), O ( $\text{sp}^2$  carbonyl oxygen, representing H-bond acceptor), N1 (neutral flat NH, like in amide, H-bond donor), and the TIP probe (molecular shape descriptor). The grid spacing was set to 0.5 Å and the CLACC (for 3D-QSAR (H<sub>3</sub>R))/or MACC2(for 3D-QSAR (HMT)) encoding with smoothing window to 0.8. The number of filtered nodes was set to 100 with 50% relative weights within the ALMOND discretization.

The interaction energy between the probe and the target molecule was calculated at each point as the sum of Lennard-Jones ( $E_{ij}$ ), hydrogen bond ( $E_{hb}$ ), electrostatic interactions ( $E_{el}$ ), and an entropic term:  $E_{xyz} = \sum E_{ij} + \sum E_{el} + \sum E_{hb} + S$  [42].

Geometry and calculated electronic properties of the target molecule have mutual impact on the interaction energy between the probe and the target molecule and consequently on the developed pharmacophore model.

The obtained maps were encoded into GRID Independent Descriptors (GRIND and GRIND2 descriptors). The GRIND and GRIND2 descriptors were independent of the alignment of the series [42]. The GRIND approach was aimed to extract the information enclosed in the MIFs and compress it into new types of variables whose values were independent of the spatial position of the molecule studied by using an optimization algorithm with the intensity of the field at a node and the mutual node–node distances between the chosen nodes as a scoring function. Such variables constituted a matrix of descriptors that were analyzed using multivariate techniques, such as principal component analysis (PCA) and partial least squares (PLS) regression analysis. The principal component analysis was used for inspection of our series and for obtaining a heatmap of our compounds describing their similarities and differences. Variables were used for development of 3D-QSAR models by use of the PLS regression [43].

Based on the PCA plots ( $t_1$  vs.  $t_2$  and  $t_1$  vs.  $u_1$ ) the data set of 35 aminoquinoline derivatives was divided on training set (27–28 compounds for QSAR models building) and verification set (7–8 compounds for QSAR models validation) [44]. The most important pharmacophores (GRID descriptors), responsible for the H<sub>3</sub>R and HMT inhibition, were selected by the PLS regression and used for the 3D-QSAR (H<sub>3</sub>R and HMT) models building (Pentacle 1.0.6 program). The formed 3D-QSAR (H<sub>3</sub>R and HMT) models and corresponding 3D-pharmacophores were used for design and selection of novel aminoquinoline derivatives as promising multipotent ligands. Quality of the obtained 3D-QSAR (H<sub>3</sub>R and HMT) models was examined by use of: leave-one-out cross-validation ( $Q^2$ ), correlation coefficient ( $R^2$  observed vs. predicted), root mean squared error of estimation (RMSEE), and external validation (root mean squared error of prediction (RMSEP)) [43,44].

Predictive power of the model was determined by  $Q^2$ , which is leave-one-out cross-validated version of  $R^2$ . A model was fitted to the data leaving one compound out, selected the best variables, and predicted  $Y$  for the left-out compound. This procedure was repeated until all compounds have been left out, which resulted in

$n$  parallel models. The difference between observed and the predicted  $Y$  values were calculated ( $e_{(i)}$ ) for each model. In this setting were defined PRESS (predicted sum of squares), RMSEP (or RMSEE) and  $Q^2$  as:

$$\text{PRESS} = \sum_{i=1}^n e_{(i)}^2 \quad (1)$$

$$\text{RMSEP} = \sqrt{\frac{\text{PRESS}}{n}} \quad (2)$$

$$Q^2 = 1 - \frac{\text{PRESS}}{\text{SSTo}} \quad (3)$$

SSTo—variation, sum of squares (total)

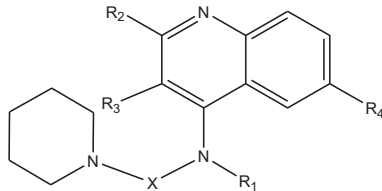
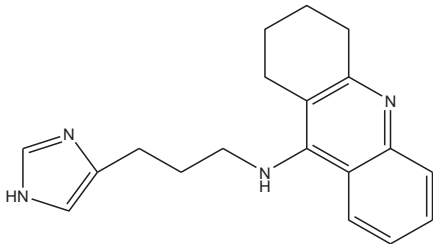
PLS models with  $Q^2 \geq 0.5$  can be considered to have good predictive capability [43–45].

Overfitting of the QSAR models was avoided by two following procedures. During the QSAR modelling the RMSE for training (RMSEE) and test (RMSEP) set were calculated and compared to each other [43,44]. The best QSAR models were selected when RMSEP of test set began to increase while RMSEE of training set continued to decrease. Also, the QSAR models with different training and test sets were compared and optimal one was chosen by comparing  $R^2$ ,  $Q^2$ , RMSEE, and RMSEP data [43,44].

Ligand-based virtual screening of Zinc database was performed of the aminoquinoline derivatives were performed against the most promising H<sub>3</sub>R/HMT ligand by use of the FLAP (fingerprints for ligands and proteins) 1.0.0 program [46].

**Table 1**

Structures and pharmacological results of the heteroaromatic-piperidine derivatives for human histamine H<sub>3</sub> receptor (H<sub>3</sub>R) and HMT inhibition [19,20].

|    |   |                               |                                    |                 |                |                                    |                         |  |
|---|---|-------------------------------|------------------------------------|-----------------|----------------|------------------------------------|-------------------------|--|
| ID  | X   | R <sub>1</sub>                | R <sub>2</sub>                     | R <sub>3</sub>  | R <sub>4</sub> | pK <sub>i</sub> (H <sub>3</sub> R) | pIC <sub>50</sub> (HMT) | pK <sub>i</sub> (H <sub>3</sub> R) + pIC <sub>50</sub> (HMT) |
| 1   | (CH <sub>2</sub> ) <sub>2</sub>   | H                             | H                                  | H               | H              | 6.72                               | 6.68                    | 13.4   |
| 2   | (CH <sub>2</sub> ) <sub>2</sub>   | CH <sub>3</sub>               | H                                  | H               | H              | 6.44                               | 6.92                    | 13.3   |
| 3   | (CH <sub>2</sub> ) <sub>2</sub>   | H                             | –(CH <sub>2</sub> ) <sub>4</sub> – | H               | 7.72           | 7.47                               | 15.2                    |  |
| 4   | (CH <sub>2</sub> ) <sub>2</sub>   | CH <sub>3</sub>               | –(CH <sub>2</sub> ) <sub>4</sub> – | H               | 7.11           | 5.85                               | 12.9                    |  |
| 5   | (CH <sub>2</sub> ) <sub>3</sub>   | H                             | H                                  | H               | H              | 7.07                               | 7.19                    | 14.3   |
| 6   | (CH <sub>2</sub> ) <sub>3</sub>   | CH <sub>3</sub>               | H                                  | H               | H              | 6.39                               | 7.80                    | 14.2   |
| 7   | (CH <sub>2</sub> ) <sub>3</sub>   | C <sub>2</sub> H <sub>5</sub> | H                                  | H               | H              | 5.95                               | 7.31                    | 13.2   |
| 8   | (CH <sub>2</sub> ) <sub>3</sub>   | H                             | H                                  | CH <sub>3</sub> | H              | 7.15                               | 6.23                    | 13.4   |
| 9   | (CH <sub>2</sub> ) <sub>3</sub>   | H                             | –(CH <sub>2</sub> ) <sub>4</sub> – | H               | 7.47           | 7.35                               | 14.8                    |  |
| 10  | (CH <sub>2</sub> ) <sub>3</sub>   | CH <sub>3</sub>               | –(CH <sub>2</sub> ) <sub>4</sub> – | H               | 7.30           | 6.44                               | 13.7                    |  |
| 11  | (CH <sub>2</sub> ) <sub>3</sub>   | H                             | –(CH) <sub>4</sub> –               | H               | 6.73           | 6.96                               | 13.7                    |  |
| 12  | (CH <sub>2</sub> ) <sub>3</sub>   | H                             | H                                  | H               | Cl             | 6.42                               | 6.70                    | 13.1   |
| 13  | (CH <sub>2</sub> ) <sub>4</sub>   | H                             | H                                  | H               | H              | 7.05                               | 7.19                    | 14.2   |
| 14  | (CH <sub>2</sub> ) <sub>4</sub>   | H                             | H                                  | H               | Cl             | 7.09                               | 6.80                    | 13.9   |
| 15  | (CH <sub>2</sub> ) <sub>5</sub>   | H                             | H                                  | H               | H              | 7.82                               | 7.28                    | 15.1   |
| 16  | (CH <sub>2</sub> ) <sub>5</sub>   | H                             | H                                  | H               | Cl             | 7.59                               | 6.85                    | 14.4   |
| 17  | (CH <sub>2</sub> ) <sub>6</sub>   | H                             | H                                  | H               | H              | 8.12                               | 7.08                    | 15.2   |
| 18  | (CH <sub>2</sub> ) <sub>6</sub>   | H                             | H                                  | CH <sub>3</sub> | H              | 8.44                               | 6.47                    | 14.9   |
| 19  | (CH <sub>2</sub> ) <sub>6</sub>   | H                             | –(CH <sub>2</sub> ) <sub>4</sub> – | H               | 8.74           | 7.68                               | 16.4                    |  |
| 20  | (CH <sub>2</sub> ) <sub>6</sub>   | H                             | H                                  | H               | Cl             | 7.74                               | 6.74                    | 14.4   |
| 21  | (CH <sub>2</sub> ) <sub>7</sub>   | H                             | H                                  | H               | Cl             | 8.00                               | 6.92                    | 14.9   |
| 22  | (CH <sub>2</sub> ) <sub>8</sub>   | H                             | H                                  | H               | Cl             | 8.11                               | 6.64                    | 14.7   |
| 23  | (CH <sub>2</sub> ) <sub>10</sub>  | H                             | H                                  | H               | Cl             | 7.92                               | 6.66                    | 14.6   |
| 24  | (CH <sub>2</sub> ) <sub>12</sub>  | H                             | H                                  | H               | Cl             | 7.49                               | 6.64                    | 14.1   |
| 25  | (CH <sub>2</sub> ) <sub>3</sub> –O–C <sub>6</sub> H <sub>4</sub> –                                | H                             | H                                  | H               |                | 10.04                              | 7.29                    | 17.3   |
| 26  | (CH <sub>2</sub> ) <sub>3</sub> –O–C <sub>6</sub> H <sub>4</sub> –                                | Cl                            | H                                  | H               |                | 10.07                              | 6.51                    | 16.6   |
| 27  | (CH <sub>2</sub> ) <sub>3</sub> –O–C <sub>6</sub> H <sub>4</sub> –(CH <sub>2</sub> ) <sub>2</sub> | H                             | H                                  | H               |                | 9.28                               | 6.92                    | 16.2   |
| 28  | (CH <sub>2</sub> ) <sub>3</sub> –O–C <sub>6</sub> H <sub>4</sub> –(CH <sub>2</sub> ) <sub>2</sub> | Cl                            | H                                  | H               |                | 9.28                               | 6.38                    | 15.7   |
| 29  | (CH <sub>2</sub> ) <sub>3</sub> –O–C <sub>6</sub> H <sub>4</sub> –(CH <sub>2</sub> ) <sub>3</sub> | H                             | H                                  | H               |                | 9.12                               | 7.51                    | 16.6   |
| 30  | (CH <sub>2</sub> ) <sub>3</sub> –O–C <sub>6</sub> H <sub>4</sub> –(CH <sub>2</sub> ) <sub>4</sub> | H                             | H                                  | H               |                | 8.82                               | 7.14                    | 15.9   |
| 31  | (CH <sub>2</sub> ) <sub>3</sub> –O–C <sub>6</sub> H <sub>4</sub> –(CH <sub>2</sub> ) <sub>2</sub> | H                             | –(CH <sub>2</sub> ) <sub>4</sub> – |                 | 9.48           | 7.32                               | 16.8                    |  |
| 32  | (CH <sub>2</sub> ) <sub>3</sub> –O–C <sub>6</sub> H <sub>4</sub> –(CH <sub>2</sub> ) <sub>3</sub> | H                             | –(CH <sub>2</sub> ) <sub>4</sub> – |                 | 8.85           | 7.02                               | 15.8                    |  |
| 33  | (CH <sub>2</sub> ) <sub>3</sub> –O–C <sub>6</sub> H <sub>4</sub> –(CH <sub>2</sub> ) <sub>4</sub> | H                             | –(CH <sub>2</sub> ) <sub>4</sub> – |                 | 8.74           | 7.32                               | 16.0                    |  |
| 34 [20] FUB770  |   |                               |                                    |                 |                | 7.03                               | 7.46                    | 14.5   |
|  |   |                               |                                    |                 |                |                                    |                         |  |
| Tacrine [19]  |   |                               |                                    |                 |                | –                                  | 6.96                    | –  |

### 3. Results and discussion

The optimized molecular models of 35 aminoquinoline derivatives along with their activity values (expressed as pKi (H<sub>3</sub>R) and pIC<sub>50</sub> (HMT)) [19,20] were loaded into the Pentacle (1.06) [39] to derive 3D-QSAR models using GRIND descriptors [42]. The H<sub>3</sub>R/HMT potency intervals were spanned 4 log units (pKi (H<sub>3</sub>R): 5.9–10.0) and 2 log units (pIC<sub>50</sub>(HMT): 5.8–7.8) in the data set (Table 1). Relatively wide H<sub>3</sub>R/HMT activity intervals of the data set provide extensive applicability domain for the formed 3D-QSAR models. The set of 35 H<sub>3</sub>R/HMT ligands includes compounds with a piperidino-alkyl (Scaffold A) or *p*-(3-piperidinopropoxy)phenyl-alkyl (Scaffold B) moiety bonded with the aminoquinoline moiety.

Since difference between pKi (H<sub>3</sub>R) and pIC<sub>50</sub> (HMT) values, pKi (H<sub>3</sub>R)–pIC<sub>50</sub>(HMT), was in most compound examples positive and spanned from –1.4 to 3.6 (Table 1), the majority of the ligands have

stronger protein binding properties for H<sub>3</sub>R than for HMT. These optimal pharmacological features of the hybrids should result in the beneficial effects on cognitive functions.

In the series of examined compounds containing a *p*-(3-piperidinopropoxy)phenyl moiety (Table 1), were determined very high affinities at H<sub>3</sub>R (Ki(H<sub>3</sub>R): 0.09–1.80 nM/pKi (H<sub>3</sub>R): 10.0–8.7) in comparison with the other reported H<sub>3</sub>R ligands [47–53]. Also, the quinoline and 1,2,3,4-tetrahydroacridine derivatives (Table 1) were about 2 and 4 times more potent HMT inhibitors than tacrine [54].

Structural variance of the data was analyzed with principal component analysis (PCA) performed on the whole set of GRIND descriptors. The first three principal components explained about 50% of the descriptor variance in the data set. Based on the PCA the data set of 35 aminoquinoline derivatives was divided on training set (27–28 compounds for QSAR models building) and Verification set (7–8 compounds for QSAR models validation) [44].

**Table 2**  
Results of the 3D-QSAR (H<sub>3</sub>R) and 3D-QSAR (HMT) modeling studies.

| Training set-H <sub>3</sub> R  |                        |                              | Training set-HMT    |                         |                               |
|--------------------------------|------------------------|------------------------------|---------------------|-------------------------|-------------------------------|
| Compound ID                    | pKi (H <sub>3</sub> R) | Pred. pKi (H <sub>3</sub> R) | Compound ID         | pIC <sub>50</sub> (HMT) | Pred. pIC <sub>50</sub> (HMT) |
| 1                              | 6.72                   | 6.59                         | 1                   | 6.68                    | 6.54                          |
| 2                              | 6.44                   | 6.43                         | 2                   | 6.92                    | 6.92                          |
| 4                              | 7.11                   | 6.99                         | 4                   | 5.85                    | outlier                       |
| 7                              | 5.95                   | 6.14                         | 5                   | 7.19                    | 7.10                          |
| 8                              | 7.15                   | 7.07                         | 6                   | 7.80                    | 7.68                          |
| 9                              | 7.47                   | 7.41                         | 7                   | 7.31                    | 7.20                          |
| 12-Dication                    | 6.42                   | 6.43                         | 8                   | 6.23                    | outlier                       |
| 12-Monocation                  | 6.42                   | 6.43                         | 9                   | 7.35                    | 7.19                          |
| 13                             | 7.05                   | 7.29                         | 10                  | 6.44                    | outlier                       |
| 14-Dication                    | 7.09                   | 7.03                         | 11                  | 6.96                    | 7.13                          |
| 14-Monocation                  | 7.09                   | 7.04                         | 12-Dication         | 6.70                    | 6.76                          |
| 16-Dication                    | 7.59                   | 7.63                         | 12-Monocation       | 6.70                    | 6.61                          |
| 16-Monocation                  | 7.59                   | 7.70                         | 13                  | 7.19                    | 7.09                          |
| 17                             | 8.12                   | 8.16                         | 14-Dication         | 6.80                    | 6.96                          |
| 18                             | 8.44                   | 8.42                         | 14-Monocation       | 6.80                    | 6.87                          |
| 19                             | 8.74                   | 8.88                         | 16-Dication         | 6.85                    | 6.74                          |
| 20-Dication                    | 7.74                   | 7.73                         | 16-Monocation       | 6.85                    | 6.85                          |
| 20-Monocation                  | 7.74                   | 7.79                         | 17                  | 7.08                    | 7.07                          |
| 21-Dication                    | 8.00                   | 7.99                         | 18                  | 6.47                    | 6.87                          |
| 21-Monocation                  | 8.00                   | 8.04                         | 19                  | 7.68                    | 7.50                          |
| 22-Dication                    | 8.11                   | 8.19                         | 20-Dication         | 6.74                    | 6.81                          |
| 22-Monocation                  | 8.11                   | 8.06                         | 20-Monocation       | 6.74                    | 6.87                          |
| 23-Dication                    | 7.92                   | 7.80                         | 21-Dication         | 6.92                    | 6.80                          |
| 23-Monocation                  | 7.92                   | 7.95                         | 21-Monocation       | 6.92                    | 6.93                          |
| 24-Dication                    | 7.49                   | 7.49                         | 22-Dication         | 6.64                    | 6.63                          |
| 24-Monocation                  | 7.49                   | 7.46                         | 22-Monocation       | 6.64                    | 6.66                          |
| 25-Dication                    | 10.04                  | 9.97                         | 23-Dication         | 6.66                    | 6.70                          |
| 25-Monocation                  | 10.04                  | 10.08                        | 23-Monocation       | 6.66                    | 6.64                          |
| 26                             | 10.07                  | 10.00                        | 24-Dication         | 6.64                    | 6.66                          |
| 27                             | 9.28                   | 9.38                         | 24-Monocation       | 6.64                    | 6.56                          |
| 28-Dication                    | 9.28                   | 9.25                         | 25-Dication         | 7.29                    | 7.28                          |
| 28-Monocation                  | 9.28                   | 9.21                         | 25-Monocation       | 7.29                    | 7.36                          |
| 30                             | 8.82                   | 8.85                         | 28-Dication         | 6.38                    | 6.31                          |
| 31                             | 9.48                   | out                          | 28-Monocation       | 6.38                    | 6.34                          |
| 32                             | 8.85                   | 8.78                         | 29                  | 7.51                    | 7.56                          |
| 34-Dication                    | 7.03                   | 7.03                         | 33                  | 7.32                    | 7.35                          |
| 34-Monocation                  | 7.03                   | 6.94                         | 34-Dication         | 7.46                    | 7.40                          |
|                                | R <sup>2</sup>         | 0.98                         | 34-Monocation       | 7.46                    | 7.53                          |
|                                | Q <sup>2</sup>         | 0.94                         | Tacrine             | 6.96                    | 7.07                          |
|                                | RMSEE                  | 0.171                        |                     | R <sup>2</sup>          | 0.80                          |
|                                |                        |                              |                     | Q <sup>2</sup>          | 0.60                          |
| <b>Test set-H<sub>3</sub>R</b> |                        |                              |                     | <b>RMSEE</b>            | 0.159                         |
| 3                              | pKi (H <sub>3</sub> R) | Pred. pKi (H <sub>3</sub> R) | <b>Test set-HMT</b> | pIC <sub>50</sub> (HMT) | Pred. pIC <sub>50</sub> (HMT) |
| 5                              | 7.72                   | 6.96                         | 3                   | 7.47                    | 6.98                          |
| 6                              | 7.07                   | 7.06                         | 15                  | 7.28                    | 6.93                          |
| 10                             | 6.39                   | 7.18                         | 26                  | 6.51                    | 6.74                          |
| 11                             | 7.30                   | 7.11                         | 27                  | 6.92                    | 7.06                          |
| 15                             | 6.73                   | 7.16                         | 30                  | 7.14                    | 7.12                          |
| 29                             | 7.82                   | 7.86                         | 31                  | 7.32                    | 7.23                          |
| 33                             | 9.12                   | 9.03                         | 32                  | 7.02                    | 7.23                          |
|                                | 8.74                   | 9.04                         |                     | <b>RMSEP</b>            | 0.262                         |
|                                | <b>RMSEP</b>           | 0.457                        |                     |                         |                               |



In order to identify the important pharmacophore features of the ligand–H<sub>3</sub>R interactions, a PLS model was built, using the complete set of active GRIND variables [42]. The FFD variables selection algorithm, implemented in Pentacle, was applied to reduce the variable number and increase the model quality. The best 3D-QSAR (H<sub>3</sub>R) model with three significant components ( $A = 3$ ),  $R^2$ : 0.98, and  $Q^2$ : 0.94, was finally created (Table 2).

Coefficient plot with the most significant variables for the H<sub>3</sub>R antagonistic potency, such as: v49: DRY–DRY, v55: DRY–DRY, v359: TIP–TIP, v457: DRY–O, v676: DRY–TIP, v877: O–TIP, v884: O–TIP, v968: N1–TIP, v341: TIP–TIP, and v846: O–TIP, is depicted on Fig. 1. The variables such as: v49: DRY–DRY, v55: DRY–DRY, v359: TIP–TIP, v457: DRY–O, v676: DRY–TIP, v877: O–TIP, v884: O–TIP, and v968: N1–TIP, are positively correlated with the H<sub>3</sub>R antagonistic activity, while variables v341: TIP–TIP and v846: O–TIP, are negatively correlated with the H<sub>3</sub>R antagonistic activity (Fig. 1).

In order to define specific pharmacophore features of the ligand–H<sub>3</sub>R interaction, the most significant GRIND variables for the H<sub>3</sub>R antagonistic activity (Fig. 1, Table 3) were compared with the most significant GRIND variables for the HMT inhibiting activity. Five specific favorable GRIND variables for the H<sub>3</sub>R antagonistic activity (v49: DRY–DRY, v55: DRY–DRY, v359: TIP–TIP, v676: DRY–TIP, v877: O–TIP, v884: O–TIP and v968: N1–TIP) could be selected (Fig. 1, Table 3). The most significant variables for H<sub>3</sub>R antagonistic activity are presented on potent H<sub>3</sub>R antagonists, compound **18** (scaffold A) (Fig. 2a) and **28** (scaffold B) (Fig. 2b).

3D-Pharmacophoric feature of compound **18** (scaffold A) mainly contains two hydrophobic quinoline and piperidine moieties at optimal distances (specific favorable v49/v55: DRY–DRY); two steric hot spots in the pyridine ring of the quinoline moiety and piperidine moiety at optimal distance (specific favorable v359: TIP–TIP); hydrophobic and steric hot spots in quinoline and piperidine moieties at optimal distance (specific favorable v676: DRY–TIP); weak H-bond acceptor piperidine ring

present at optimal distance from a steric hot spot in quinoline moiety (specific favorable v968: N1–TIP); H-bond donor quinoline N-group present at optimal distance (v877: O–TIP) from a steric hot spot in piperidine moiety (v877: O–TIP), and H-bond donor quinoline N-group present at optimal distance from a steric hot spot in piperidine moiety (v884: O–TIP) (Fig. 2a, Table 3).

3D-Pharmacophoric feature of compound **28** (scaffold B) contains two hydrophobic quinoline and piperidine moieties at optimal distance (specific favorable v49/v55: DRY–DRY); two steric hot spots in the pyridine ring of the quinoline moiety and piperidine moiety at optimal distance (specific favorable v359: TIP–TIP); hydrophobic and steric hot spots in quinoline and piperidine moieties at optimal distance (specific favorable v676: DRY–TIP), strong H-bond acceptor O-bridge present at optimal distance from a steric hot spot of quinoline moiety (specific favorable v968: N1–TIP); H-bond donor quinoline N-group present at optimal distance from a steric hot spot in piperidine moiety (v877: O–TIP), and H-bond donor piperidine N-group present at optimal distance from a steric hot spot in quinoline moiety (v884: O–TIP) (Fig. 2b, Table 3).

Both compounds **18** (scaffold A) and **28** (scaffold B) contain two significant variables, v341: TIP–TIP—related to steric hot spots in the quinoline and benzen moieties and v846: O–TIP—related to H-bond donor amino group present at specific distance from steric hot spot of quinoline moiety, which negatively correlate with the hH<sub>3</sub>R antagonistic activity (Fig. 2a and b, Table 3).

3D-pharmacophoric feature of compound **18** (scaffold A) mainly differs from 3D pharmacophoric feature of compound **28** (scaffold B) in values of v968: N1–TIP specific favorable GRIND variables for H<sub>3</sub>R antagonistic activity. The v968: N1–TIP is formed between weak H-bond acceptor piperidine ring present at distance from a steric hot spot in quinoline moiety in compound **18** (Fig. 2a), while in compound **28** v968: N1–TIP is created between strong H-bond acceptor O-bridge present at optimal distance from a steric hot spot of quinoline moiety (Fig. 2b, Table 3). The difference in v968: N1–TIP values between 3D-pharmacophore of scaffold A

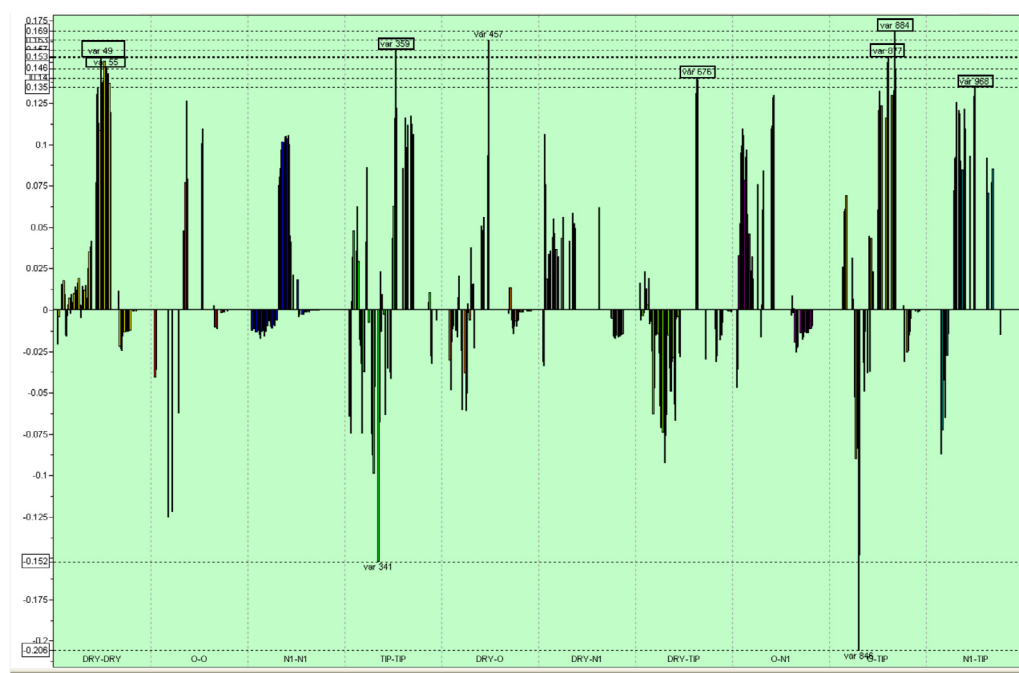


**Fig. 1.** PLS-coefficient plot and the most important GRIND variables showing the descriptors directly (positive value) or inversely (negative values) correlated to pKi (H<sub>3</sub>R). The H<sub>3</sub>R antagonistic activity particularly increases with the increase in (DRY–DRY), (DRY–O), (DRY–TIP), and (N1–TIP) descriptor value. The specific GRIND variables of the 3D-QSAR (H<sub>3</sub>R) model are marked in squares.

**Table 3**

Summary of GRIND variables and their corresponding distances identified as being highly correlated to H<sub>3</sub>R antagonistic/HMT inhibiting activities of examined compounds. The specific GRIND variables of the H<sub>3</sub>R antagonistic/HMT inhibiting activity are bolded.

| H <sub>3</sub> R-Variable | Distance [Å] | Correlogram/influence on H <sub>3</sub> R | H <sub>3</sub> R pharmacophores—comments   | HMT-variable | Distance [Å] | Correlogram/influence on HMT | HMT pharmacophores—comments   |
|---------------------------|--------------|---|--|--------------|--------------|------------------------------|---|
| <b>V49</b>                | 19.6–20.0    | DRY–DRY/+                                 | <b>Optimal</b> distance separating hydrophobic quinoline and piperidine moieties<br>Pronounced in all B scaffold ligands and A scaffold compounds with spacer (X) of more than 5 methylene groups  | <b>V119</b>  | 6.8–7.2      | O–O/–                        | <b>Related</b> to two close H-bond donor groups, piperidine N-group and amino/or methylene group of back chain<br>Pronounced in all ligands except compounds <b>6, 7, 18, 19, 29, 34</b> , tacrine  |
| <b>V55</b>                | 22.0–22.4    | DRY–DRY/+                                 | <b>Optimal</b> distance separating hydrophobic quinoline and piperidine moieties<br>Pronounced in all B scaffold ligands and A scaffold compounds with spacer (X) of more than 6 methylene groups  | <b>V125</b>  | 9.2–9.6      | O–O/–                        | <b>Related</b> to two close H-bond donor groups, quinoline N-group and amino group of back chain<br>Pronounced in all ligands except compounds <b>6, 22, 23, 24, 29</b>   |
| V341                      | 14.0–14.4    | TIP–TIP/–                                 | Related to two steric hot spots in the quinoline moiety<br>Pronounced in all ligands except compound 17 and 30   | <b>V140</b>  | 15.2–15.6    | O–O/+                        | <b>Optimal</b> distance separating two H-bond donor groups, N-group of quinoline/or amino group of back chain and piperidine moiety<br>Pronounced in all B scaffold ligands and A scaffold ligands except compounds <b>2, 7, 16, 17, 18</b> |
| <b>V359</b>               | 21.2–21.6    | TIP–TIP/+                                 | <b>Optimal</b> distance separating two steric hot spots in the pyridine ring of the quinoline moiety and piperidine moiety<br>Pronounced in all B scaffold ligands, and almost all A scaffold ligands except compounds <b>2, 7, 23</b> , and <b>24</b>         | <b>V312</b>  | 2.4–2.8      | TIP–TIP/–                    | <b>Related</b> to steric hot spot in substituent of the quinoline moiety<br>Pronounced in all ligands   |
| V457                      | 19.6–20.0    | DRY–O/+                                   | H-bond donor, piperidine N-group or amino group, present far away from a hydrophobic hot spot, quinoline or piperidine moiety respectively<br>Pronounced in all B scaffold ligands and A scaffold ligands except compounds <b>1, 2</b> , and <b>7</b>          | V340         | 13.4–14.0    | TIP–TIP/–                    | Related to two steric hot spots in the quinoline moiety<br>Pronounced in all ligands  |
| <b>V676</b>               | 25.6–26.0    | DRY–TIP/+                                 | <b>Optimal</b> distance separating hydrophobic and steric hot spots in quinoline and piperidine moieties<br>Pronounced in all B scaffold ligands and A scaffold compounds with spacer (X) of more than 5 methylene groups                                      | <b>V361</b>  | 22.0–22.4    | TIP–TIP/–                    | <b>Related</b> to steric hot spot in quinoline moiety present far away from a steric hot spot in piperidine moiety<br>Pronounced in all ligands except compounds <b>2, 6, 7, 23, 24, 34</b> , tacrine                                       |
| V846                      | 12.0–12.4    | O–TIP/–                                   | H-bond donor, piperidine N-group or amino group, present quite near to a steric hot spot, quinoline or piperidine moiety respectively<br>Pronounced in all ligands   | V453         | 18.0–18.4    | DRY–O/+                      | H-bond donor, piperidine N-group or amino group, present far away from a hydrophobic hot spot, quinoline or piperidine moiety respectively<br>Pronounced in all ligands except tacrine  |
| <b>V877</b>               | 24.4–24.8    | O–TIP/+                                   | H-bond donor, piperidine N-group or quinoline N-group, present far away from a steric hot spot in quinoline or piperidine moiety respectively<br>Pronounced in all B scaffold ligands and A scaffold compounds with spacer (X) of more than 5 methylene groups | <b>V678</b>  | 26.4–26.8    | DRY–TIP/–                    | <b>Related</b> to hydrophobic hot spot of piperidine ring present far away from a steric hot spot in quinoline moiety<br>Pronounced in all ligands with B scaffold and A scaffold compounds with spacer (X) longer than 5 methylene groups  |
| <b>V884</b>               | 27.2–27.6    | O–TIP/+                                   | H-bond donor, piperidine N-group or quinoline N-group, present far away from a steric hot spot in quinoline or piperidine moiety respectively<br>Pronounced in all B scaffold ligands and A scaffold compounds with spacer (X) of more than 5 methylene groups | V845         | 11.6–12.0    | O–TIP/–                      | H-bond donor, piperidine N-group or amino group, present quite near to a steric hot spot, quinoline or piperidine moiety respectively<br>Pronounced in all ligands  |
| <b>V968</b>               | 20.0–20.4    | N1–TIP/+                                  | <b>H-bond acceptor</b> , piperidine ring or O-bridge, present far away from a steric hot spot in quinoline moiety<br>Pronounced in all B scaffold ligands and A scaffold ligands with spacer (X) of less than 10 or more than 5 methylene groups               | <b>V867</b>  | 20.4–20.8    | O–TIP/+                      | <b>H-bond donor</b> , piperidine N-group or quinoline N-group, present far away from a steric hot spot in quinoline or piperidine moiety respectively<br>Pronounced in all ligands except compounds <b>1, 2, 7</b> , tacrine                |

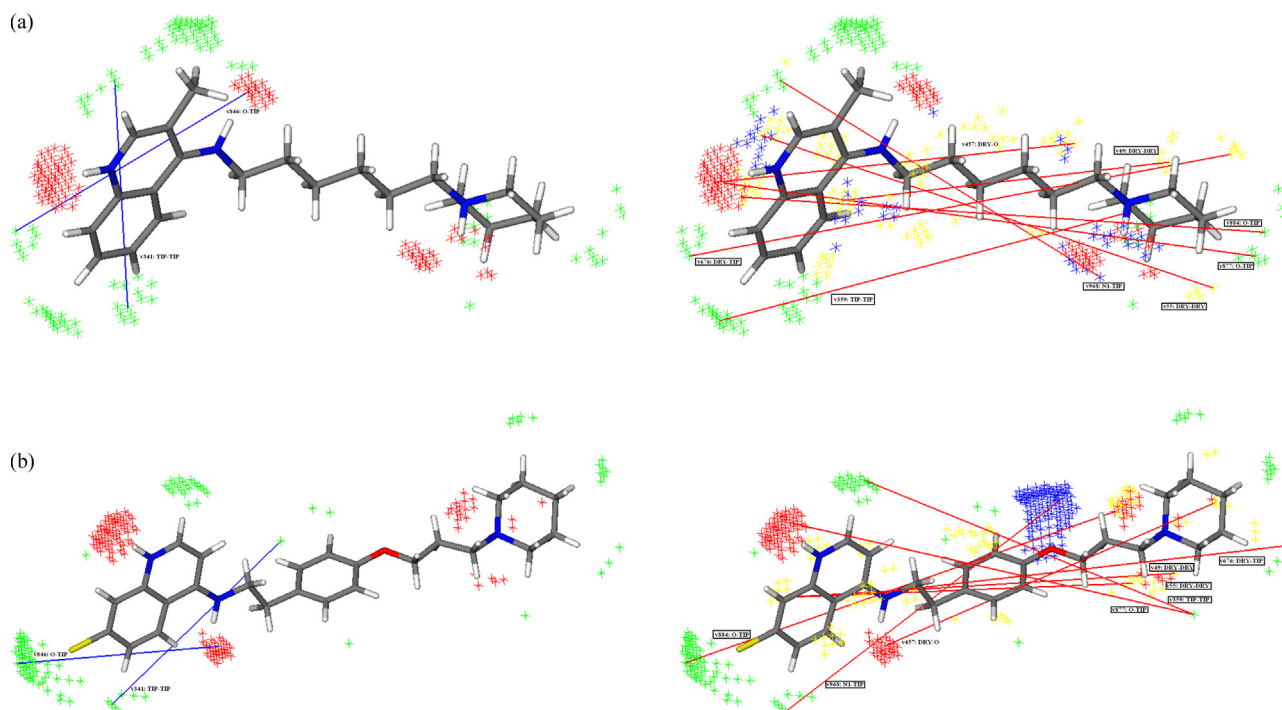


**Fig. 2.** (a) 3D-Pharmacophoric feature of compound **18** (scaffold A) for  $H_3R$  antagonistic activity. (b) 3D-Pharmacophoric feature of compound **28** (scaffold B) for  $H_3R$  antagonistic activity. The hydrophobic hot spots (DRY) are presented in yellow, steric hot spots TIP are depicted in green, H-bond donor regions (O) are presented in red, and H-bond acceptor regions (N1) are depicted in blue. Favorable interactions are presented in red and unfavorable interactions are presented in blue. The specific GRIND variables of the  $H_3R$  antagonistic activity are marked in squares. (For interpretation of the references to color in this figure legend, the reader is referred to the web version of this article.)

ligands and scaffold B ligands is responsible for significantly stronger  $H_3R$  antagonistic activity of scaffold B ligands.

Unfavorable GRIND variables for  $H_3R$  antagonistic activity (v341: TIP–TIP and v846: O–TIP) are present in all examined ligands (Table 3, Fig. 2). The specific favorable GRIND variables for  $H_3R$  antagonistic activity (v49: DRY–DRY, v55: DRY–DRY, v359:

TIP–TIP, v676: DRY–TIP, v877: O–TIP, v884: O–TIP, and v968: N1–TIP; Table 3) are present in all B scaffold ligands and in A scaffold ligands with spacer (X) of less than 10 or more than 5 methylene groups (Fig. 2). Condensation of quinoline moiety with cyclohexan ring of scaffold A/B ligands with shorter spacer (X), like compounds pairs **1/3**, **2/4**, **5/9**, **6/10**, **17/19**, **27/31**, resulted in increase of the

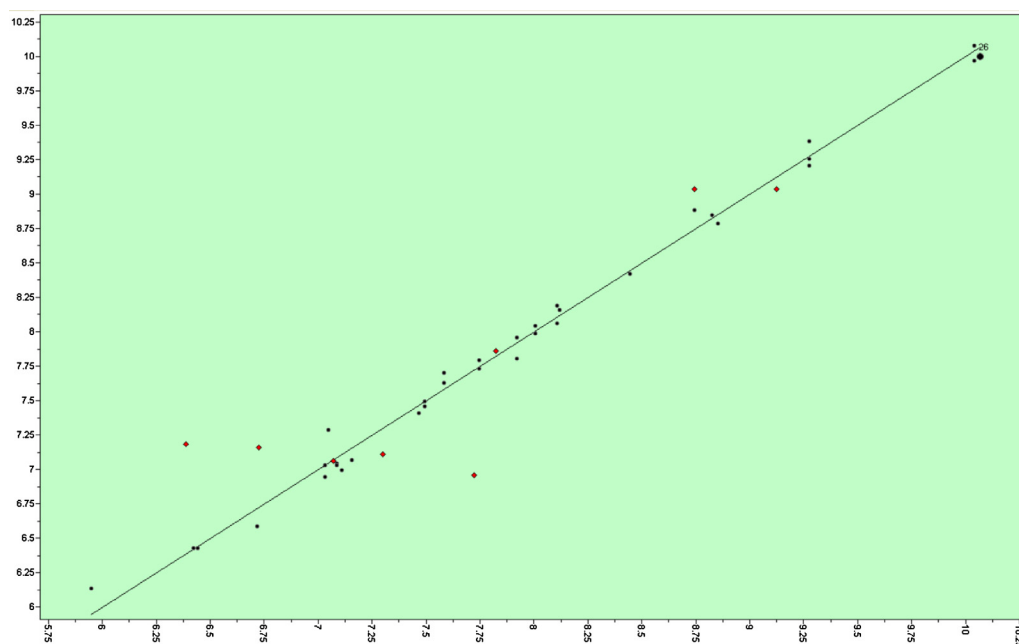


**Fig. 3.** Observed vs. predicted  $pK_i$  ( $H_3R$ ) antagonistic activities for training and test set.



**Table 4**Results of external validation of 3D-QSAR ( $H_3R$ ) model [56,57].

| Test set-1- $H_3R$ [56] |                |                      | Test set-2- $H_3R$ [57]   |                |                      |
|-------------------------|----------------|----------------------|---------------------------|----------------|----------------------|
| Compound ID [Ref.]      | pKi ( $H_3R$ ) | Pred. pKi ( $H_3R$ ) | Compound ID [Ref.]        | pKi ( $H_3R$ ) | Pred. pKi ( $H_3R$ ) |
| <b>3</b>                | 8.77           | 8.06                 | <b>1</b>                  | 8.85           | 8.89                 |
| <b>4c (cis)</b>         | 9.52           | 8.75                 | <b>2</b>                  | 8.30           | 8.30                 |
| <b>4t (trans)</b>       | 9.68           | 8.45                 | <b>3</b>                  | 8.05           | 8.45                 |
| <b>5c (cis)</b>         | 9.47           | 8.72                 | <b>4</b>                  | 8.32           | 7.40                 |
| <b>5t (trans)</b>       | 9.60           | 9.18                 | <b>5</b>                  | 8.75           | 9.37                 |
| <b>6c (cis)</b>         | 9.48           | 9.06                 | <b>6</b>                  | 8.60           | 7.96                 |
| <b>6t (trans)</b>       | 9.60           | 9.25                 | <b>7</b>                  | 8.44           | 8.78                 |
| <b>7t (trans)</b>       | 9.19           | 9.31                 | <b>8</b>                  | 8.80           | 7.87                 |
| <b>8c (cis)</b>         | 9.25           | 9.26                 | <b>9</b>                  | 8.55           | 8.36                 |
| <b>9c (cis)</b>         | 9.04           | 9.83                 | <b>10</b>                 | 8.31           | 7.71                 |
| <b>9t (trans)</b>       | 9.50           | 9.85                 | <b>11</b>                 | 8.28           | 8.72                 |
| <b>10c (cis)</b>        | 9.17           | 9.54                 | <b>12</b>                 | 8.08           | 8.71                 |
| <b>10t (trans)</b>      | 9.39           | 9.00                 | <b>13</b>                 | 8.44           | 8.61                 |
| <b>11c (cis)</b>        | 9.04           | 8.84                 | <b>14</b>                 | 8.66           | 7.57                 |
| <b>11t (trans)</b>      | 9.24           | 8.60                 | <b>15</b>                 | 8.80           | 7.93                 |
| <b>12c (cis)</b>        | 9.39           | 8.92                 | <b>16</b>                 | 7.98           | 9.86                 |
| <b>12t (trans)</b>      | 9.77           | 9.33                 | <b>17</b>                 | 9.70           | 8.79                 |
| <b>13c (cis)</b>        | 9.54           | 9.26                 | <b>ABT239</b>             | 9.35           | 8.86                 |
| <b>13t (trans)</b>      | 9.59           | 8.94                 | <b>FUB2.922</b>           | 8.52           | 8.09                 |
| <b>14c (cis)</b>        | 9.28           | 9.85                 | <b>RMSEP/test set-2</b>   |                | 0.743                |
| <b>14t (trans)</b>      | 9.19           | 9.11                 |                           |                |                      |
| <b>15t (trans)</b>      | 8.50           | 9.38                 |                           |                |                      |
| <b>16t (trans)</b>      | 8.26           | 7.40                 |                           |                |                      |
| <b>JNJ-5207852</b>      | 9.22           | 8.83                 |                           |                |                      |
| <b>RMSEP/test set-1</b> |                | 0.579                | <b>RMSEP/test set-1-2</b> |                | 0.657                |

specific favorable GRIND variables (v49: DRY-DRY, v55: DRY-DRY, v359: TIP-TIP, v676: DRY-TIP, and v968: N1-TIP) and stronger  $H_3R$  antagonistic activity.

Involvement of hydrophobic hot spots of quinoline and piperidine moieties in three specific favorable GRIND variables for  $H_3R$  antagonistic activity (v49: DRY-DRY, v55: DRY-DRY, and v676: DRY-TIP) indicated that introduction of lipophilic substituent in quinoline/piperidine rings and/or saturation of double bonds in quinoline ring will increase lipophilicity of the rings and enhance  $H_3R$  antagonistic activity.

Also, two significant favorable GRIND variables for  $H_3R$  antagonistic activity between piperidine N-group present at optimal distance (24.4–24.8 Å (v877: O-TIP) and 27.2–27.6 Å (v884: O-TIP)) from a steric hot spot in quinoline moiety are pronounced in all B scaffold ligands and A scaffold compounds with spacer (X) of more than 5 methylene groups (Table 3). Since the specific favorable variable v676: DRY-TIP, significant favorable variable v877: O-TIP, and significant favorable variable v884: O-TIP are formed between piperidine moiety present very far away (24.4–27.6 Å) from a steric hot spot in quinoline ring of the ligands

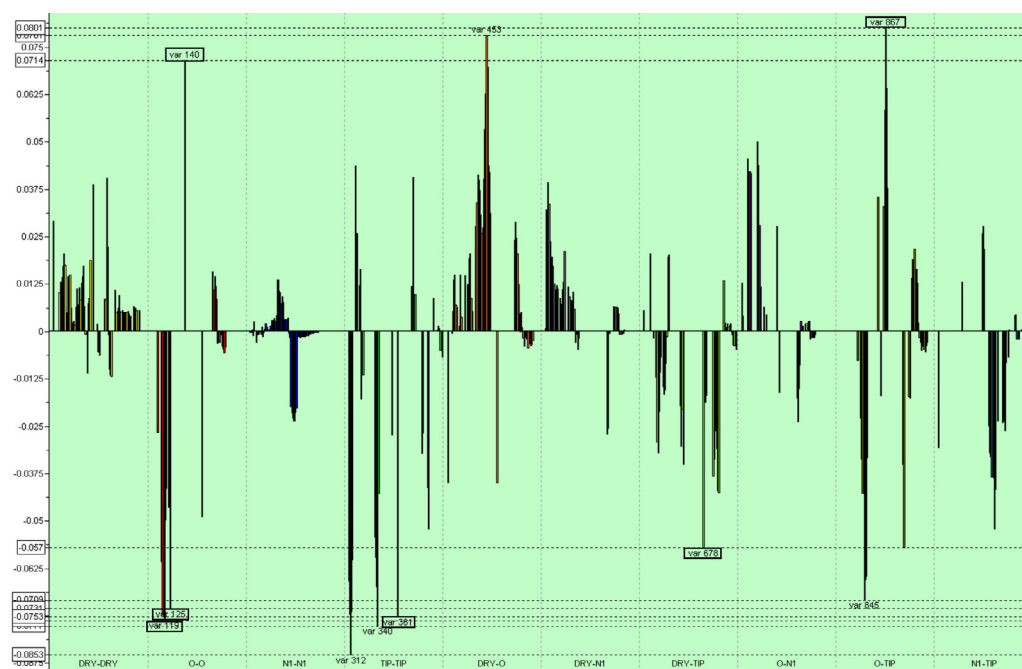


**Fig. 4.** PLS-coefficient plot and the most important GRIND variables showing the descriptors directly (positive value) or inversely (negative values) correlated to  $pIC_{50}(HMT)$ . The HMT inhibitory potency particularly increases with the increase in (DRY-O) descriptor value and with decrease in (TIP-TIP) and (DRY-TIP) descriptor values. The specific GRIND variables of the 3D-QSAR (HMT) model are marked in squares.

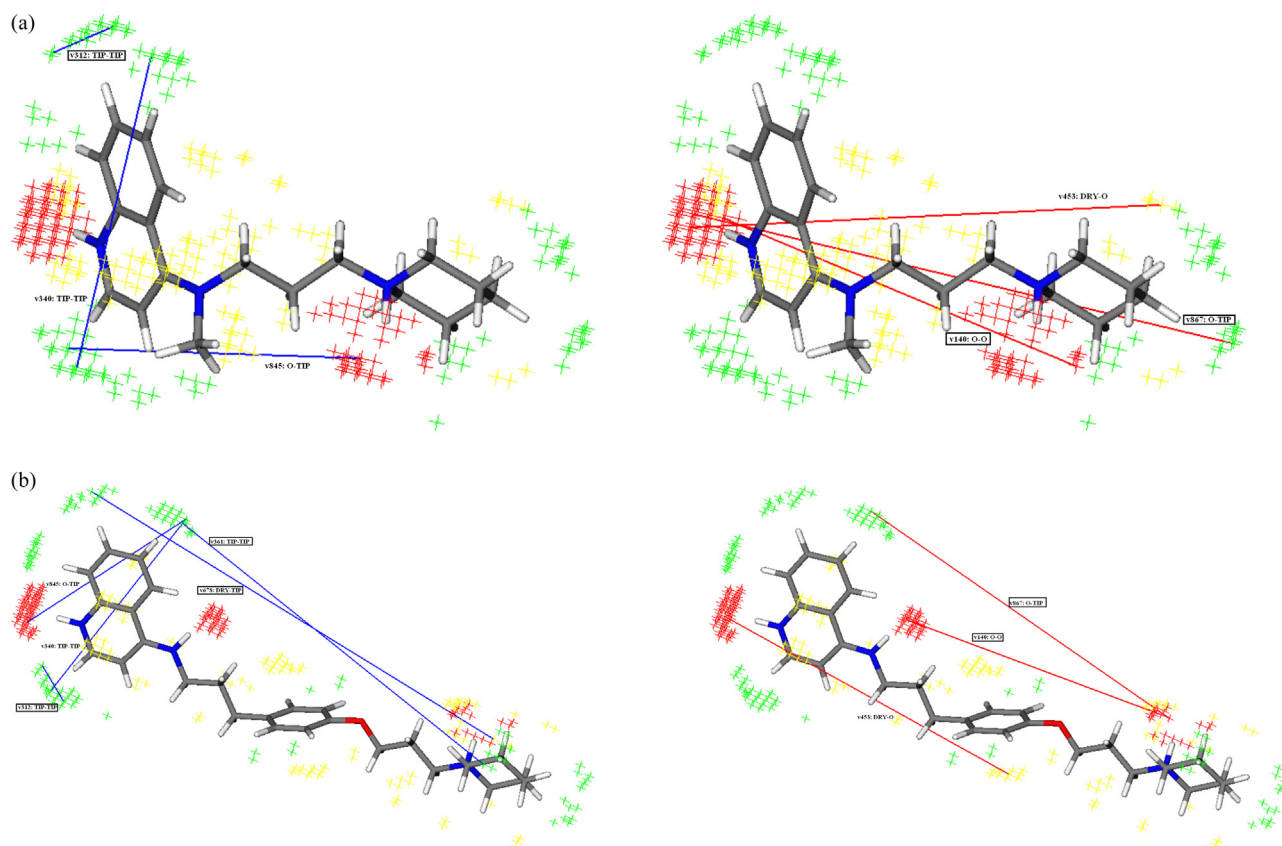


**Fig. 5.** (a) 3D-Pharmacophoric feature of compound **6** (scaffold A) for HMT inhibiting activity. (b) 3D-Pharmacophoric feature of compound **29** (scaffold B) for HMT inhibiting activity. The hydrophobic hot spots (DRY) are presented in yellow, steric hot spots TIP are depicted in green, H-bond donor regions (O) are presented in red, and H-bond acceptor regions (N1) are depicted in blue. Favorable interactions are presented in red and unfavorable interactions are presented in blue. The specific GRIND variables of the HMT inhibiting activity are marked in squares. (For interpretation of the references to color in this figure legend, the reader is referred to the web version of this article.)

can be concluded that potent H<sub>3</sub>R antagonists should contain longer spacer between piperidine and quinoline rings.

Since the tertiary amine of the piperidine moiety forms ionic interactions with Asp114 in transmembrane domain III of the H<sub>3</sub>R the basic piperidine moiety is essential for receptor binding and responsible for maintenance of binding properties at H<sub>3</sub>R [55]. This finding is in agreement with two significant favorable GRIND variables for H<sub>3</sub>R antagonistic activity (Table 3) between piperidine N-group present at optimal distance (24.4–24.8 Å (v877: O–TIP) and 27.2–27.6 Å (v884: O–TIP)) from a steric hot spot in quinoline moiety. Therefore, introduction of electron donating substituent in piperidine ring of the A/B scaffold ligands will increase basic properties of the piperidine moiety and thereby, enhance H<sub>3</sub>R antagonistic activity.

Predictive potential of the developed 3D-QSAR (H<sub>3</sub>R) model was tested by use of leave-one-out cross validation of the training set

( $Q^2$ : 0.94 and RMSEE: 0.171) and verification set (RMSEP: 0.457) (Table 2). The statistical and validation parameters indicated that the 3D-QSAR (H<sub>3</sub>R) model has good prognostic capacity for H<sub>3</sub>R antagonistic activity of the related aminoquinoline derivatives (Fig. 3).

In order to test reliability of the 3D-QSAR (H<sub>3</sub>R) model for predicting H<sub>3</sub>R activities of ligands with different chemical scaffolds, two test sets (H<sub>3</sub>R) of significantly different structures than training set compounds (Supplement material), were subjected to the 3D-QSAR study.

For test set-1 (H<sub>3</sub>R) of 24 cyclohexylamine-based ligands (Supplement material) [56] were predicted pKi (H<sub>3</sub>R) values with RMSEP 0.574, while for test set-2 (H<sub>3</sub>R) of 19 FUB2.922 derivatives, with various heterocyclic moieties (Supplement material) [57] were predicted pKi (H<sub>3</sub>R) values with RMSEP 0.743. Total RMSEP for both test sets was 0.657. In the test sets (H<sub>3</sub>R) were also included three very potent and clinically relevant H<sub>3</sub>R ligands: FUB2.922 [57], JNJ-5207852 [58] and ABT 239 [59].

Considering a large Y-domain (4.5 log units) of the 3D-QSAR (H<sub>3</sub>R) model (Table 2), the RMSEE 0.171 for training set (Table 2), the RMSEP 0.457 for related test set (Table 2), and the RMSEP 0.657 for the external test sets of structurally different compounds (Table 4), could be concluded that the 3D-QSAR (H<sub>3</sub>R) model is reliable and widely applicable predicting tool for evaluation of various H<sub>3</sub>R ligands.

The best 3D-QSAR (HMT) model with three significant components ( $A = 3$ ),  $R^2$ : 0.80, and  $Q^2$ : 0.60, was formed by use of the Pentacle 1.0.6 program (Table 2). Coefficient plot with the most significant variables for the HMT inhibiting activity, such as: v119: O–O, v125: O–O, v140: O–O, v312: TIP–TIP, v340: TIP–TIP, v361:

**Table 5**  
Results of external validation of 3D-QSAR (HMT) model [21].

| Test set-HMT     |                              |                               |
|------------------|------------------------------|-------------------------------|
| Compound ID [21] | pIC <sub>50</sub> (HMT) [21] | Pred. pIC <sub>50</sub> (HMT) |
| <b>12</b>        | 7.62                         | 7.17                          |
| <b>13</b>        | 7.10                         | 7.27                          |
| <b>14</b>        | 7.07                         | 7.22                          |
| <b>16</b>        | 7.46                         | 7.19                          |
| <b>15</b>        | 7.46                         | 7.36                          |
| <b>11</b>        | 7.26                         | 7.24                          |
| <b>17</b>        | 6.27                         | 7.14                          |
| <b>FUB 854</b>   | 7.47                         | 6.71                          |
| <b>RMSEP</b>     |                              | 0.455                         |

TIP–TIP, v453: DRY–O, v678: DRY–TIP, v845: O–TIP, and v867: O–TIP, is shown on Fig. 3. The variables such as: v140: O–O, v453: DRY–O, and v867: O–TIP, are positively correlated with the HMT inhibiting activity, while variables v119: O–O, v125: O–O, v312: TIP–TIP, v340: TIP–TIP, v361: TIP–TIP, v678: DRY–TIP, and v845: O–TIP, are negatively correlated with the HMT inhibiting activity (Fig. 3).

In order to define specific pharmacophore features of the ligand–HMT interaction, the most significant GRIND variables for the H<sub>3</sub>R antagonistic activity (Fig. 1, Table 3) were compared with the most significant GRIND variables for the HMT inhibiting activity (Fig. 4, Table 3). The specific GRIND variables (v119: O–O, v125: O–O, v140: O–O, v312: TIP–TIP, v361: TIP–TIP, v678: DRY–TIP, and v867: O–TIP) significant for the HMT inhibiting activity are marked (Fig. 4, Table 3).

The most significant variables for HMT inhibiting activity are presented on potent HMT inhibitors, compound **6** (scaffold A) (Fig. 5a) and **29** (scaffold B) (Fig. 5b).

3D-Pharmacophoric feature of compound **6** (scaffold A) contains two H-bond donor groups of quinoline and piperidine moieties at optimal distance (specific favorable v140: O–O) and H-bond donor group of quinoline ring at optimal distance from a steric hot spot in piperidine moiety (specific favorable v867: O–TIP) (Fig. 5a, Table 5). Compound **6** contains three specific unfavorable variables for HMT inhibiting activity: v312: TIP–TIP related to two steric hot spots in substituent of the quinoline moiety at specific distance, v340: TIP–TIP related to steric hot spots in quinoline moiety, and v845: O–TIP between H-bond donating piperidine N-group and steric hot spots of quinoline moiety (Fig. 5a, Table 3).

3D-Pharmacophoric feature of compound **29** (scaffold B) contains two H-bond donors, amino group of back chain and piperidine moiety, at optimal distance of (specific favorable v140: O–O) and H-bond donor group of piperidine ring present at optimal distance from a steric hot spot in quinoline moiety (specific favorable v867: O–TIP) (Fig. 5b, Table 3). Compound **29** contains five specific unfavorable variables for HMT inhibiting activity: v312: TIP–TIP related to two steric hot spots in substituent of the quinoline moiety, v340: TIP–TIP related to steric hot spots in

quinoline moiety, v361: TIP–TIP related to steric hot spot in quinoline moiety present far away from a steric hot spot in piperidine moiety, v678: DRY–TIP related to hydrophobic hot spot of piperidine ring present very far away from a steric hot spot in quinoline moiety, and v845: O–TIP between H-bond donating quinoline N-group and steric hot spots of quinoline moiety (Fig. 5b, Table 3). Since the specific unfavorable variable v678: DRY–TIP is formed between piperidine moiety present very far away from a steric hot spot in quinoline ring of the ligands is concluded that potent HMT inhibitors should contain shorter spacer between piperidine and quinoline moieties.

Three unfavorable GRIND variables for HMT inhibiting activity, v312: TIP–TIP, v340: TIP–TIP, and v845: O–TIP, are present in all examined ligands (Table 3, Fig. 5).

Since the significant favorable variables for HMT inhibiting activity (v140: O–O, v453: DRY–O, and v867: O–TIP) contain H-bond donor groups of quinoline, amino group of back chain and piperidine moieties (Fig. 5) structural modifications of the A/B scaffold ligands that increase basic properties of the quinoline, amino group of back chain and piperidine ring could result in enhanced HMT inhibiting activity. Therefore substitution in quinoline/piperidine rings with electron donating substituents and/or saturation of double bonds in quinoline ring are recommended as optimal structural modifications for stronger HMT inhibiting activity of the examined ligands.

Based on the crystal structure of HMT in complex with inhibitor diphenhydramine (PDB: 2AOT) were selected essential polar interactions with three catalytic residues Glu28, Gln143, and Asn283 for inhibitors binding [60]. The terminal nitrogen atom of amine group of the diphenhydramine extends toward the polar end of Glu28 and forms a hydrogen bond, while Y-shaped hydrophobic-ring structure of diphenhydramine contacts aromatic residues from different regions (Phe9, Tyr146, Tyr147, Trp179, Trp183, Tyr198, and Phe243) [60]. These findings are in agreement with selected significant favorable variables for HMT inhibiting activity: specific favorable GRIND variable (v140: O–O) between two H-bond donor groups of quinoline/or amino group of back chain and piperidine moieties at optimal distance 15.2–15.6 Å, favorable GRIND variable (v453: DRY–O) between piperidine N-

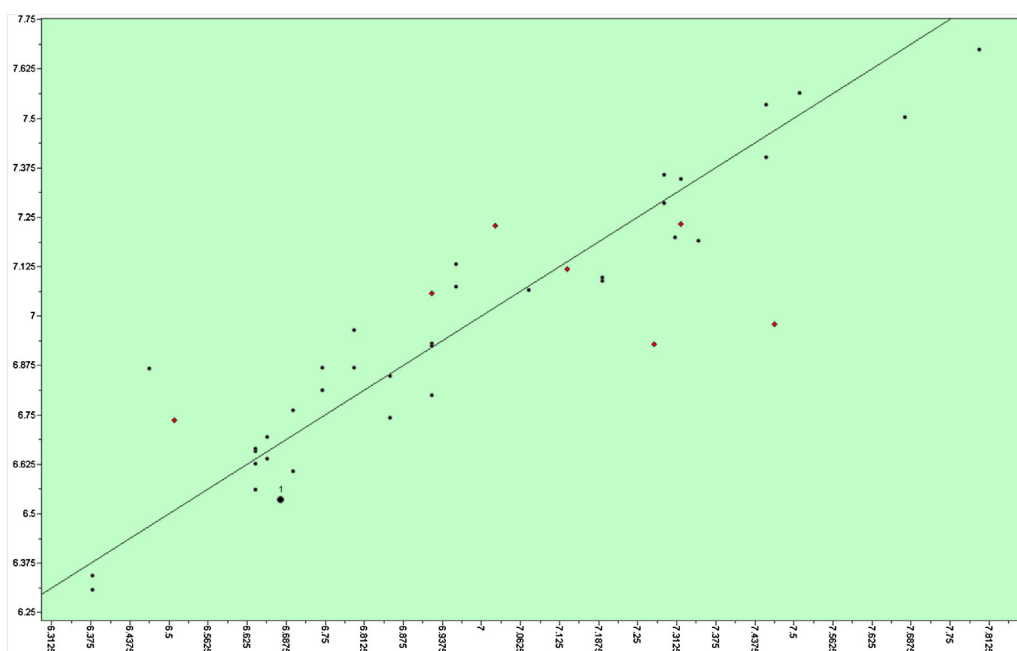


Fig. 6. Observed vs. Predicted  $pIC_{50}(\text{HMT})$  inhibiting activities for training and test set.

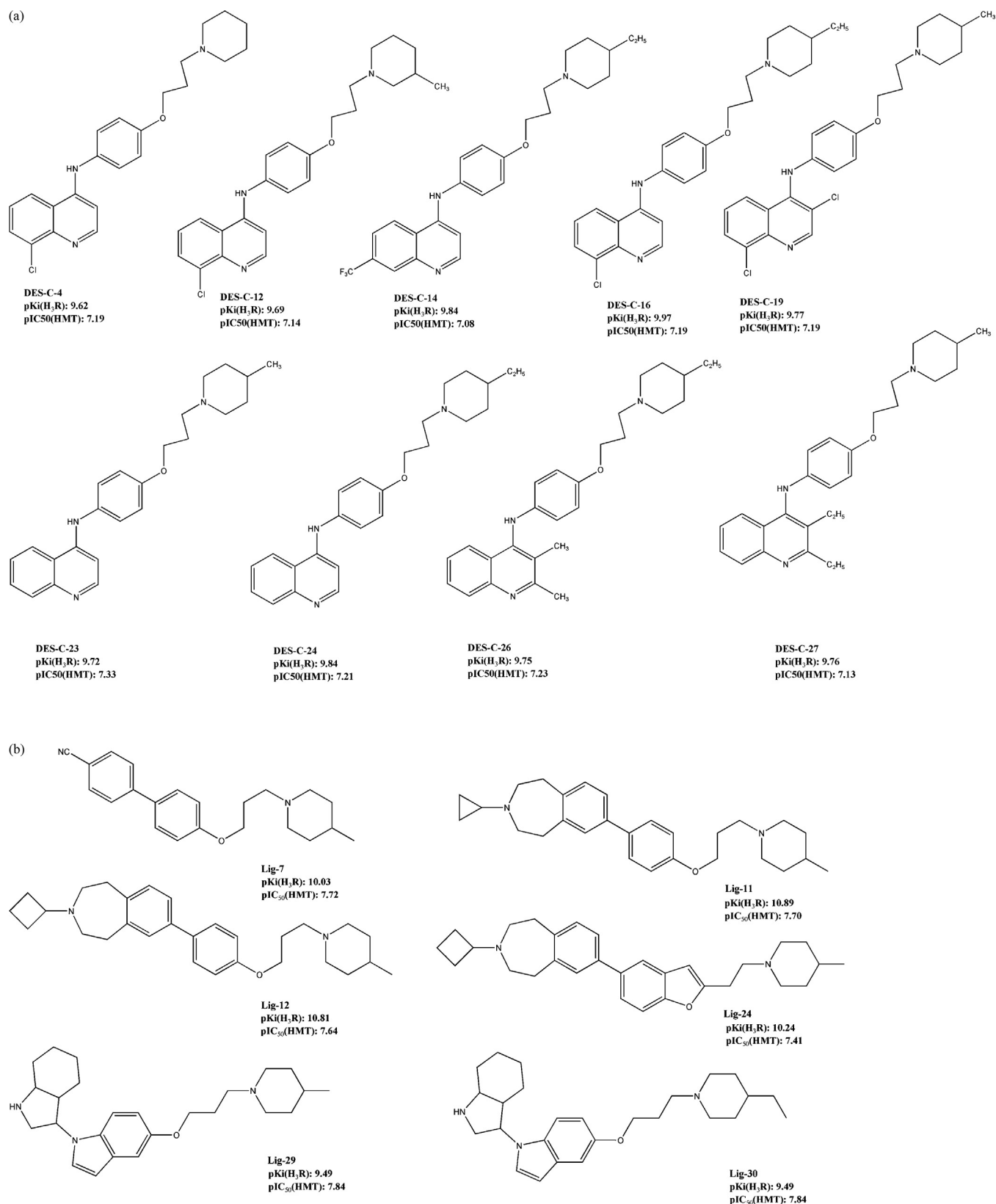


Fig. 7. Designed H<sub>3</sub>R/HMT ligands with optimal H<sub>3</sub>R/HMT activities and ADMET properties.

group or amino group at optimal distance 18.0–18.4 Å from a hydrophobic hot spot of quinoline or piperidine moiety respectively, and specific favorable GRIND variable (v867: O-TIP) between H-bond donor group of piperidine N-group or quinoline

N-group at optimal distance 20.4–20.8 Å from a steric hot spot in quinoline or piperidine moiety respectively.

Predictive potential of the developed 3D-QSAR (HMT) model was tested by use of leave-one-out cross validation of the training

set ( $Q^2$ : 0.60 and RMSEE: 0.159) and verification set (RMSEP: 0.262) (Table 2). The statistical and validation parameters indicated that the 3D-QSAR (HMT) model could be applied for predicting HMT inhibiting activity of the related aminoquinoline derivatives (Fig. 6).

Reliability of the 3D-QSAR (HMT) model for evaluation of structurally diverse HMT inhibitors was tested on external test set (HMT) of ligands with significantly different structures than training set compounds (Supplement material).

Test set (HMT) was created from imidazole-containing HMT ligands, with experimentally observed inhibiting activities  $IC_{50}(\text{HMT}) < 1 \mu\text{M} \equiv pIC_{50}(\text{HMT}) > 6$  (Supplement material) [21]. Because only several compounds from the data set [21] are relatively potent HMT inhibitors ( $IC_{50}(\text{HMT}) < 1 \mu\text{M}$ ,  $pIC_{50}(\text{HMT}) > 6$ ) the external test set (HMT) was formed from 8 HMT ligands. The 3D-QSAR (HMT) model was predicted  $pIC_{50}(\text{HMT})$  values for the external test set (HMT) with RMSEP 0.455 (Table 5). Acceptable accuracy of the predicted  $pIC_{50}(\text{HMT})$  values was confirmed by good ratio between RMSEE 0.159 for the training set (Table 2), the RMSEP 0.262 for related test set (Table 2), and the RMSEP 0.455 for the test set (HMT) of structurally different ligands (Table 5). Therefore the 3D-QSAR (HMT) model was proposed for further drug design studies as reliable tool in  $pIC_{50}(\text{HMT})$  evaluation for various related compounds.

3D-pharmacophoric feature for  $H_3R$  antagonistic activity (v49: DRY-DRY, v55: DRY-DRY, v359: TIP-TIP, v676: DRY-TIP, v877: O-TIP, v884: O-TIP and v968: N1-TIP) mainly differs from 3D-pharmacophoric feature for HMT inhibiting activity (v140: O-O and v867: O-TIP) in: specific lipophilic/steric components of the  $H_3R$  pharmacophore (v49: DRY-DRY, v55: DRY-DRY, v359: TIP-TIP, v676: DRY-TIP) H-bond accepting components of the  $H_3R$  pharmacophore (v968: N1-TIP), H-bond donating components of the HMT pharmacophore (v140: O-O), longer optimal distance between H-bond donor and steric hot spots of the  $H_3R$  pharmacophore (v877: O-TIP (24.4–24.8 Å), v884: O-TIP (27.2–27.6 Å)) than of HMT pharmacophore (v867: O-TIP (20.4–20.8 Å)), and specific presence of favorable interaction between hydrophobic and very far away steric hot spots in the  $H_3R$  pharmacophore (v676: DRY-TIP (25.6–26.0 Å)).

Since the  $H_3R$ -pharmacophore (v676: DRY-TIP, v877: O-TIP, v884: O-TIP (24.4–27.6 Å)) differ from HMT-pharmacophore (v867: O-TIP, 20.4–20.8 Å) in optimal distance between piperidine moiety and steric hot spot in quinoline ring, multipotent  $H_3R$ /HMT ligands should contain a medium length spacer between the piperidine and quinoline rings as in structures of compound **19** (scaffold A) and compound **25** (scaffold B) (Supplement Fig. 1).

Because of significantly stronger  $H_3R$  antagonistic activity of compound **25** (scaffold B) than compound **19** (scaffold A) structure of the compound **25** is used as lead for design of novel multipotent  $H_3R$ /HMT ligands.

The created 3D-pharmacophore models ( $H_3R$ /HMT) were further applied for design of novel derivatives of lead compound **25** (Supplement material). The 3D-QSAR ( $H_3R$ ) and 3D-QSAR (HMT) models were used for  $pKi$  ( $H_3R$ ) and  $pIC_{50}(\text{HMT})$  activity prediction for the designed ligands. The designed compounds with 3D-QSAR predicted  $pKi$  ( $H_3R$ )  $> 9.6$  and ( $pKi$  ( $H_3R$ ) +  $pIC_{50}(\text{HMT})$ )  $> 16.8$ , **Des-C4**, **Des-C12**, **Des-C16**, **Des-C23**, **Des-C24**, **Des-C26**, **Des-C27**, were selected for further synthesis (Fig. 7, Table 6). The chosen compounds mainly differ in predicted  $pKi$  ( $H_3R$ ) values, while  $pIC_{50}(\text{HMT})$  is spanned in very narrow interval (7.16–7.36). The predicted  $pKi$  ( $H_3R$ ) for the **Des-C4**, **Des-C12**, and **Des-C16** ligands (Table 6) indicated on very favorable influence of methyl/ethyl substituent at *para* position of the piperidine ring on  $H_3R$  activity. These results are in accordance with 3D-pharmacophore for  $H_3R$  (v49: DRY-DRY, v55: DRY-DRY,

**Table 6**

3D-QSAR predicted  $H_3R$  ( $pKi$ ) and HMT ( $pIC_{50}$ ) activities for the designed aminoquinoline derivatives.

| Designed compounds | Predicted $pKi$ ( $H_3$ ) | Predicted $pIC_{50}$ (HMT) | $pKi$ ( $H_3$ ) + $pIC_{50}$ (HMT) | $pKi$ ( $H_3$ ) – $pIC_{50}$ (HMT) |
|--------------------|---------------------------|----------------------------|------------------------------------|------------------------------------|
| Des-C1             | 8.86                      | 7.23                       | 16.1                               | 1.6                                |
| Des-C2             | 9.52                      | 7.22                       | 16.7                               | 2.3                                |
| Des-C3             | 9.33                      | 7.22                       | 16.6                               | 2.1                                |
| <b>Des-C4</b>      | <b>9.62</b>               | 7.19                       | <b>16.8</b>                        | 2.4                                |
| Des-C5             | 9.36                      | 7.14                       | 16.5                               | 2.2                                |
| Des-C6             | 9.48                      | 7.13                       | 16.6                               | 2.4                                |
| Des-C7             | 9.37                      | 7.24                       | 16.6                               | 2.1                                |
| Des-C8             | 9.39                      | 7.32                       | 16.7                               | 2.1                                |
| Des-C9             | 8.83                      | 7.25                       | 16.1                               | 1.6                                |
| Des-C10            | 9.35                      | 7.02                       | 16.4                               | 2.3                                |
| Des-C11            | 9.16                      | 7.24                       | 16.4                               | 1.9                                |
| <b>Des-C12</b>     | <b>9.69</b>               | 7.14                       | <b>16.8</b>                        | 2.6                                |
| Des-C13            | 9.46                      | 7.05                       | 16.5                               | 2.4                                |
| <b>Des-C14</b>     | <b>9.84</b>               | 7.08                       | <b>16.9</b>                        | 2.8                                |
| Des-C15            | 9.35                      | 7.12                       | 16.5                               | 2.2                                |
| <b>Des-C16</b>     | <b>9.97</b>               | 7.19                       | <b>17.2</b>                        | 2.8                                |
| Des-C17            | 9.30                      | 7.05                       | 16.4                               | 2.3                                |
| Des-C18            | 9.24                      | 7.21                       | 16.5                               | 2.0                                |
| <b>Des-C19</b>     | <b>9.77</b>               | 7.19                       | <b>17.0</b>                        | 2.6                                |
| Des-C20            | 9.48                      | 7.08                       | 16.6                               | 2.4                                |
| Des-C21            | 9.37                      | 7.23                       | 16.6                               | 2.1                                |
| Des-C22            | 9.30                      | 7.30                       | 16.6                               | 2.0                                |
| <b>Des-C23</b>     | <b>9.72</b>               | <b>7.33</b>                | <b>17.1</b>                        | 2.4                                |
| <b>Des-C24</b>     | <b>9.84</b>               | <b>7.21</b>                | <b>17.1</b>                        | 2.6                                |
| Des-C25            | 9.44                      | 7.20                       | 16.6                               | 2.2                                |
| <b>Des-C26</b>     | <b>9.75</b>               | <b>7.23</b>                | <b>17.0</b>                        | 2.5                                |
| <b>Des-C27</b>     | <b>9.76</b>               | <b>7.13</b>                | <b>16.9</b>                        | 2.6                                |
| Des-C28            | 9.36                      | 7.07                       | 16.4                               | 2.3                                |
| Des-C29            | 9.11                      | 7.27                       | 16.4                               | 1.8                                |
| Des-C30            | 9.14                      | 7.45                       | 16.6                               | 1.7                                |
| Des-C31            | 8.49                      | 7.33                       | 15.8                               | 1.2                                |
| Des-C32            | 8.53                      | 7.34                       | 15.9                               | 1.2                                |
| Des-C33            | 8.21                      | 7.29                       | 15.5                               | 0.9                                |

**Table 7**

3D-QSAR predicted  $H_3R$  ( $pKi$ ) and HMT ( $pIC_{50}$ ) activities for the designed  $H_3R$ /HMT ligands of various chemical scaffolds.

| Designed Compounds | Predicted $pKi$ ( $H_3$ ) | Predicted $pIC_{50}$ (HMT) | $pKi$ ( $H_3$ ) + $pIC_{50}$ (HMT) | $pKi$ ( $H_3$ ) – $pIC_{50}$ (HMT) |
|--------------------|---------------------------|----------------------------|------------------------------------|------------------------------------|
| Lig-1              | 8.77                      | 7.38                       | 16.14                              | 1.39                               |
| Lig-2              | 8.96                      | 7.16                       | 16.12                              | 1.80                               |
| Lig-3              | 9.07                      | 7.48                       | 16.55                              | 1.59                               |
| Lig-4              | 9.23                      | 7.43                       | 16.66                              | 1.80                               |
| Lig-5              | 9.01                      | 7.47                       | 16.48                              | 1.54                               |
| Lig-6              | 9.17                      | 7.29                       | 16.46                              | 1.88                               |
| <b>Lig-7</b>       | <b>10.03</b>              | 7.72                       | <b>17.75</b>                       | 2.31                               |
| Lig-8              | 8.87                      | 6.93                       | 15.80                              | 1.93                               |
| Lig-9              | 9.34                      | 7.77                       | 17.11                              | 1.57                               |
| Lig-10             | 9.27                      | 7.45                       | 16.72                              | 1.83                               |
| <b>Lig-11</b>      | <b>10.89</b>              | 7.70                       | <b>18.59</b>                       | 3.19                               |
| <b>Lig-12</b>      | <b>10.81</b>              | 7.64                       | <b>18.45</b>                       | 3.17                               |
| Lig-13             | 8.53                      | 7.29                       | 15.82                              | 1.25                               |
| Lig-14             | 8.56                      | 7.21                       | 15.77                              | 1.36                               |
| Lig-15             | 8.40                      | 7.39                       | 15.80                              | 1.01                               |
| Lig-16             | 8.90                      | 7.55                       | 16.45                              | 1.36                               |
| Lig-1              | 8.73                      | 7.31                       | 16.04                              | 1.42                               |
| Lig-18             | 9.15                      | 7.42                       | 16.57                              | 1.73                               |
| Lig-19             | 8.46                      | 7.03                       | 15.49                              | 1.44                               |
| Lig-20             | 8.61                      | 6.89                       | 15.50                              | 1.73                               |
| Lig-21             | 8.74                      | 7.38                       | 16.13                              | 1.36                               |
| Lig-22             | 9.19                      | 7.41                       | 16.59                              | 1.78                               |
| Lig-23             | 8.83                      | 7.08                       | 15.91                              | 1.75                               |
| <b>Lig-24</b>      | <b>10.24</b>              | 7.41                       | <b>17.65</b>                       | 2.83                               |
| Lig-25             | 8.58                      | 7.27                       | 15.84                              | 1.31                               |
| Lig-26             | 8.68                      | 7.21                       | 15.89                              | 1.47                               |
| Lig-27             | 9.19                      | 7.67                       | <b>16.85</b>                       | 1.52                               |
| Lig-28             | 8.92                      | 7.56                       | 16.48                              | 1.37                               |
| <b>Lig-29</b>      | <b>9.49</b>               | <b>7.84</b>                | <b>17.33</b>                       | 1.65                               |
| <b>Lig-30</b>      | <b>9.49</b>               | <b>7.84</b>                | <b>17.33</b>                       | 1.65                               |



v359: TIP–TIP, v676: DRY–TIP, v877: O–TIP, and v884: O–TIP) antagonistic activities.

Designed compounds **Des-C23**, **Des-C24**, **Des-C26**, and **Des-C27** differ in presence of methyl/ethyl substituent at *para* position of the piperidine ring and methyl/ethyl substituent in quinoline moiety. From the predicted  $pK_i$  ( $H_3R$ ) activities of the ligands is concluded that presence of ethyl/methyl substituent at *para* position of the piperidine moiety together with two methyl/ethyl substituents in the quinoline ring have the strongest influence on enhanced  $H_3R$  activities of the **Des-C26** and **Des-C27** compounds. These results are in accordance with 3D-pharmacophore for  $H_3R$  (v49: DRY–DRY, v55: DRY–DRY, v359: TIP–TIP, v676: DRY–TIP, v877: O–TIP, v884: O–TIP, and v968: N1–TIP) activity (Table 3).

Several examined 1,2,3,4-tetrahydroacridine derivatives (**5**, **9**, **11**, **31–34**), with similar structural features to tacrine, showed inhibitory potencies on AChE and BChE too [20]. These integrated pharmacological features of the hybrids should act synergistically or additively on the improvement of cognitive functions. Linear relationships between  $pK_i$  ( $H_3R$ )– $pIC_{50}$ (AChE) and  $pK_i$  ( $H_3R$ )– $pIC_{50}$ (BChE) activities of the ligands (**5**, **9**, **11**, **31–34**) were obtained with correlation coefficients  $r$ : 0.60. Also, very high correlation coefficient  $r$ : 0.97 was obtained for  $pIC_{50}$ (AChE)– $pIC_{50}$ (BChE) activities of the compounds (Supplement Table 1). This  $H_3R$ /HMT/AChE/BChE multitarget profile of 1,2,3,4-tetrahydroacridine derivatives (**5**, **9**, **11**, **31–34**) indicated on possible integrated pharmacological features of the designed compounds **Des-C26** and **Des-C27** with two methyl/ethyl substituents in the quinoline ring (Fig. 7), but the exact computational profiling on all these targets is beyond the scope of this study.

Many highly potent and selective  $H_3R$  antagonists were in preclinical development as procognitive agents [57,59] but were not advanced for clinical evaluation due to hERG channel affinity and cardiotoxicity [61]. Since the common pharmacophore for  $H_3R$  antagonists contains a basic amine linked to an aromatic moiety [13], introduction of a second amine moiety away from the aromatic part increases  $H_3R$  binding affinity [19,62] and in same time significantly reduces hERG affinity [57]. Based on these new findings and our pharmacophore models we designed set of 30 very diverse dibasic compounds, characterized by a two basic centers linked to an aromatic core (Supplement material). The 3D-QSAR ( $H_3R$ ) and 3D-QSAR (HMT) models were used for  $pK_i$  ( $H_3R$ ) and  $pIC_{50}$ (HMT) activity prediction for the designed ligands. The designed compounds with 3D-QSAR predicted  $pK_i$  ( $H_3R$ ) > 9.6 and  $(pK_i$  ( $H_3R$ ) +  $pIC_{50}$ (HMT)) > 16.8, **Lig-7**, **Lig-11**, **Lig-12**, **Lig-24**, **Lig-29**, **Lig-30**, were selected for further synthesis (Fig. 7, Table 7).

Finally, ADMET Predictor v. 6.5 [63] and ACD-Lab [64] programs are applied for ADMET properties evaluation of the lead compound **25** and the selected designed compounds, **Des-C23**, **Des-C24**, **Des-C26**, **Des-C27**, **Lig-7**, **Lig-11**, **Lig-12**, **Lig-24**, **Lig-29**, and **Lig-30**, (Supplement Table 2). For the designed compounds **Des-C26**, **Des-C27**, **Lig-11**, and **Lig-12**, are predicted brain penetration sufficient for CNS activity, while the lead compound **25** is defined as CNS inactive due to the low brain penetration [58] (Supplement Fig. 2). Also, for the designed compound **Des-C26**, **Lig-11**, and **Lig-12** are estimated lower hERG toxicity, toxicity risk, and metabolic CYP risk than for the lead compound **25** (Supplement Table 2).

The hybrid compounds with (sub)nanomolar activities on the both  $H_3R$  and HMT targets [19,20] are able to increase inter-synaptic histamine levels in the CNS, via  $H_3R$  autoreceptors blockade and reduced catabolic rate for histamine inactivation via HMT inhibition [20,22,23], and lead to beneficial procognitive effects in psychiatric and neurodegenerative diseases [10,19–23]. Also, dibasic dual  $H_3R$  antagonists/inverse agonists–AChE inhibitors have been proposed for therapy of AD [65–67]. Based on

the results we have assumed that selected **Des-C26**, **Lig-11**, and **Lig-12** compounds could lead to beneficial procognitive therapeutic effects.

Finally, ligand based virtual screening (LB-VS) of ZINC database (<http://zinc.docking.org/>) is performed against the most promising  $H_3R$ /HMT ligand, compound **25**. Top ranked **50** compounds (Supplement material), with total score >1.4, are tested by both 3D-QSAR models (Supplement Table 3). Average 3D-QSAR predicted values for the tested compounds,  $pK_i$  ( $H_3R$ ): 6.7 and  $pIC_{50}$ (HMT): 6.8, indicate on good agreement between 3D-QSAR and LB-VS results.

#### 4. Conclusions

The set of 35 multipotent  $H_3R$ /HMT ligands, containing piperidino and aminoquinoline moiety, were examined by the 3D-QSAR approach with goal to define essential chemical features for  $H_3R$  antagonism and HMT inhibition, design potent  $H_3R$ /HMT ligands, and predict  $pK_i$  ( $H_3R$ )/ $pIC_{50}$ (HMT) activities of the designed compounds.

Strong H-bond acceptor O-bridge present at optimal distance (20.0–20.4 Å) from a steric hot spot of quinoline moiety (v968: N1–TIP) was selected to be responsible for significantly stronger  $H_3R$  antagonistic activity of scaffold B ligands than scaffold A ligands.

Structure of the  $H_3R$ -pharmacophore indicated that increase of quinoline/piperidine rings lipophilicity and stronger basic properties of the piperidine moiety could enhance  $H_3R$  antagonistic activity, while the HMT-pharmacophore indicated that stronger basic properties of the quinoline/piperidine rings could augment HMT inhibiting activity of the ligands.

Since the  $H_3R$ -pharmacophore differ from HMT-pharmacophore in optimal distance between piperidine moiety and steric hot spot in quinoline ring multipotent  $H_3R$ /HMT ligands should contain a medium length spacer between the piperidine and quinoline rings as compound **19** (scaffold A) and compound **25** (scaffold B) derivatives.

The created 3D-pharmacophore models ( $H_3R$ /HMT) were applied for design and evaluation of novel ligands. For designed compounds (**Des-C26**, **Des-C27**, **Lig-11**, and **Lig-12**), with 3D-QSAR predicted  $pK_i$  ( $H_3R$ ) > 9.6 and  $(pK_i$  ( $H_3R$ ) +  $pIC_{50}$ (HMT)) > 16.8 and optimal ADMET profile, were selected as novel candidates which should act synergistically or additively on the improvement of cognitive functions.

The LB-VS of ZINC database against compound **25** selected **50** compounds as potential ligands of both targets.

#### Conflict of interest statement

All authors confirm to not have no involvement that might potentially pose conflict of interest.

#### Acknowledgements

KN and DA acknowledge project supported by the Ministry of Education, Science and Technological Development of the Republic of Serbia, Project number 172033. Further supports by Else Kröner-Fresenius-Stiftung, Translational Research Innovation–Pharma (TRIP), Fraunhofer-Projektgruppe für Translationale Medizin und Pharmakologie (TMP) (to HS) and the European COST Actions BM1007, CM1103, and CM1207 are also kindly acknowledged.

#### Appendix A. Supplementary data

Supplementary data associated with this article can be found, in the online version, at 10.1016/j.jtice.2014.09.017.



## References

- [1] Schwartz JC, Arrang JM, Garbarg M, Pollard H, Ruat M. Histaminergic transmission in the mammalian brain. *Physiol Rev* 1991;71:1–51.
- [2] Brown RE, Stevens DR, Haas HL. The physiology of brain histamine. *Prog Neurobiol* 2001;63:637–72.
- [3] Arrang JM, Garbarg M, Schwartz JC. Auto-inhibition of brain histamine release mediated by a novel class ( $H_3$ ) of histamine receptor. *Nature* 1983;302:832–7.
- [4] Humbert-Claude M, Morisset S, Gbahou F, Arrang JM. Histamine.  $H_3$  and dopamine D2 receptor-mediated [ $^{35}$ S]GTP- $\gamma$ [S] binding in rat striatum: evidence for additive effects but lack of interactions. *Biochem Pharmacol* 2007;73:1172–81.
- [5] Garduno-Torres B, Trevino M, Gutierrez R, Arias-Montano JA. Presynaptic histamine  $H_3$  receptors regulate glutamate, but not GABA release in rat thalamus. *Neuropharmacology* 2007;52:527–35.
- [6] Dai H, Fu Q, Shen Y, Hu W, Zhang Z, Timmerman H, et al. The histamine  $H_3$  receptor antagonist clobenpropit enhances GABA release to protect against NMDA induced excitotoxicity through the cAMP/protein kinase A pathway in cultured cortical neurons. *Eur J Pharmacol* 2007;563:117–23.
- [7] Threlfell S, Cragg SJ, Imre K, Turi GF, Coen CW, Greenfield SA. Histamine  $H_3$  receptors inhibit serotonin release in substantia nigra pars reticulata. *J Neurosci* 2004;24:8704–10.
- [8] Gemkow MJ, Davenport AJ, Harich S, Ellenbroek BA, Cesura A, Hallett D. The histamine  $H_3$  receptor as a therapeutic drug target for CNS disorders. *Drug Discov Today* 2009;14:509–15.
- [9] Esbenshade TA, Browman KE, Bitner RS, Strakhova M, Cowart MD, Brioni JD. The histamine  $H_3$  receptor: an attractive target for the treatment of cognitive disorders. *Br J Pharmacol* 2008;154:1166–81.
- [10] Sander K, Kottke T, Stark H. Histamine  $H_3$  receptor antagonists go to clinics. *Biol Pharm Bull* 2008;31:2163–81.
- [11] Stocking EM, Letavic MA. Histamine.  $H_3$  antagonists as wake-promoting and pro-cognitive agents. *Curr Top Med Chem* 2008;8:988–1002.
- [12] Letavic MA, Barbier AJ, Dvorak CA, Carruthers NI. Recent medicinal chemistry of the histamine  $H_3$  receptor. *Prog Med Chem* 2006;44:181–206.
- [13] Celanire S, Wijtmans M, Talaga P, Leurs R, de Esch IJP. Keynote review: histamine  $H_3$  receptor antagonists reach out for the clinic. *Drug Discov Today* 2005;10:1613–27.
- [14] Letavic MA, Aluisio L, Attack JR, Bonaventure P, Carruthers NI, Dugovic C, et al. Pre-clinical characterization of aryloxypropylidene amides as histamine  $H_3$  receptor antagonists: identification of candidates for clinical development. *Bioorg Med Chem Lett* 2010;20:4210–4.
- [15] Hancock AA, Fox GB. Perspectives on cognitive domains,  $H_3$  receptor ligands and neurological disease. *Expert Opin Investig Drugs* 2004;13:1237–48.
- [16] Passani MB, Lin JS, Hancock A, Crochet S, Blandina P. The histamine  $H_3$  receptor as a novel therapeutic target for cognitive and sleep disorders. *Trends Pharmacol Sci* 2004;25:618–25.
- [17] Vohora D. Histamine-selective  $H_3$  receptor ligands and cognitive function: an overview. *IDrugs* 2004;7:667–73.
- [18] Fox MD, Snyder AZ, Vincent JL, Corbetta M, Van Essen DC, Raichle ME. The human brain is intrinsically organized into dynamic, anticorrelated functional networks. *Proc Natl Acad Sci USA* 2005;102:9673–8.
- [19] Apelt J, Ligneau X, Pertz H, Arrang JM, Ganellin CR, Schwartz JC, et al. Development of a new class of non-imidazole histamine  $H_3$  receptor ligands with combined inhibitory histamine  $N$ -methyltransferase activity. *J Med Chem* 2002;45:1128–41.
- [20] Petroianu G, Arafat K, Sasse BC, Stark H. Multiple enzyme inhibitions by histamine  $H_3$  receptor antagonists as potential procognitive agents. *Pharmazie* 2006;61:179–82.
- [21] Grassmann S, Apelt J, Sippl W, Ligneau X, Pertz HH, Zhao YH, et al. Imidazole derivatives as a novel class of hybrid compounds with inhibitory histamine  $N$ -methyltransferase potencies and histamine  $H_3$  receptor affinities. *Bioorg Med Chem* 2003;11:2163–74.
- [22] Grassmann S, Apelt J, Ligneau X, Pertz HH, Arrang JM, Schwartz JC, et al. Search for histamine  $H_3$  receptor ligands with combined inhibitory potency at histamine  $N$ -methyltransferase: omega-piperidinoalkylamine derivatives. *Arch Pharm* 2004;337:533–45.
- [23] Apelt J, Grassmann S, Ligneau X, Pertz HH, Ganellin CR, Arrang JM, et al. Search for histamine  $H_3$  receptor antagonists with combined inhibitory potency at  $N$ -methyltransferase: ether derivatives. *Pharmazie* 2005;60:97–106.
- [24] Ligneau X, Lin JS, Vanni-Mercier G, Jouvett M, Muir JL, Ganellin CR, et al. Neurochemical and behavioural effects of Ciproxifan, a potent histamine  $H_3$ -receptor antagonist. *J Pharmacol Exp Ther* 1998;287:658–66.
- [25] Berlin M, Boyce CW, de Lera Ruiz M. Histamine  $H_3$  receptor as a drug discovery target. *J Med Chem* 2011;54:26–53.
- [26] Celanire S, Wijtmans M, Talaga P, Leurs R, de Esch IJP. Histamine  $H_3$  receptor antagonists reach out for the clinic. *Drug Discov Today* 2005;10:1613–27.
- [27] Cowart M, Altenbach R, Black L, Faghieh R, Zhao C, Hancock AA. Medicinal chemistry and biological properties of non-imidazole histamine  $H_3$  antagonists. *Mini Rev Med Chem* 2004;4:979–92.
- [28] Stephanos JJ. Drug-protein interactions: Two-site binding of heterocyclic ligands to a monomeric hemoglobin. *J Inorg Biochem* 1996;62:155–69.
- [29] Papp-Jambor C, Jaschinski U, Forst H. Cytochrome p450 enzymes and their role in drug interactions. *Anaesthesiol* 2002;51:2–15.
- [30] Zhang M, Ballard ME, Pan L, Roberts S, Faghieh R, Cowart M, et al. Lack of cataleptogenic potentiation with non-imidazole  $H_3$  receptor antagonists reveals potential drug–drug interactions between imidazole-based  $H_3$  receptor antagonists and antipsychotic drugs. *Brain Res* 2005;1045:142–9.
- [31] ChemAxon. MarvinSketch 5.5.1.0 program. Budapest, Hungary: ChemAxon; 2011. ([www.chemaxon.com/products.html](http://www.chemaxon.com/products.html)).
- [32] Froese Fischer CF. The Hartree–Fock method for atoms: a numerical approach. New York, NY: John Wiley and Sons; 1977.
- [33] Frisch MJ, et al. Gaussian 98 (revision A.7). Pittsburgh, PA: Gaussian, Inc.; 1998.
- [34] Filipic S, Nikolic K, Vovk I, Krizman M, Agbaba D. Quantitative structure–mobility relationship analysis of imidazoline receptor ligands in CDs-mediated CE. *Electrophoresis* 2013;34:471–82.
- [35] Nikolic K, Ivković B, Bešović Ž, Marković S, Agbaba D. A validated enantio-specific method for determination and purity assay of clobiprogrel. *Chirality* 2009;21:878–85.
- [36] Remko M, Swart M, Bickelhaupt M. Theoretical study of structure, pKa, lipophilicity, solubility, absorption and polar surface area of some centrally acting antihypertensives. *Bioorg Med Chem* 2006;14:1715–28.
- [37] Nikolic K, Filipic S, Agbaba D. QSAR study of imidazoline antihypertensive drugs. *Bioorg Med Chem* 2008;16:7134–40.
- [38] Nikolic K, Filipic S, Agbaba D. QSAR study of selective I1-imidazoline receptor ligands. *SAR QSAR Environ Res* 2008;20:133–44.
- [39] Molecular Discovery Ltd. Pentacle, version 1.0.6. Perugia, Italy: Molecular Discovery Ltd; 2009. ([http://www.moldiscovery.com/soft\\_pentacle.php](http://www.moldiscovery.com/soft_pentacle.php)).
- [40] Schrödinger, LLC. LigPrep, version 2.5. New York, NY: Schrödinger, LLC; 2011.
- [41] Schrödinger, LLC. Phase, version 3.3. New York, NY: Schrödinger, LLC; 2011.
- [42] Schrödinger, LLC. Maestro, version 9.2. New York, NY: Schrödinger, LLC; 2011.
- [43] Pastor M, Cruciani G, McLay I, Pickett S, Clementi S. GRIND-INdependent. Descriptors (GRIND): a novel class of alignment-independent three-dimensional molecular descriptors. *J Med Chem* 2000;43:3233–43.
- [44] Eriksson L, Johansson E, Kettaneh-Wold N, Trygg J, Wikström C, Wold S, editors. Multi- and megavariate data analysis. Basic principles and applications I. 2nd ed., Umeå: Umetrics Academy; 2001.
- [45] Tropsha A. Best practices for QSAR model development, validation, and exploitation. *Mol Inf* 2010;29:476–88.
- [46] Wold S, Johansson E, Cocchi M. In: Kubinyi H, editor. 3D-QSAR in drug design, theory, methods, and applications. Leiden: ESCOM Science Publishers; 1993 p. 523–50.
- [47] Molecular Discovery Ltd. FLAP (fingerprints for ligands and proteins), version 1.0.0. Perugia, Italy: Molecular Discovery Ltd; 2012. ([http://www.moldiscovery.com/soft\\_flap.php](http://www.moldiscovery.com/soft_flap.php)).
- [48] Lazewska D, Kuder K, Ligneau X, Schwartz JC, Schunack W, Stark H, et al. Piperidine variations in search for non-imidazole histamine  $H_3$  receptor ligands. *Bioorg Med Chem* 2008;16:8729–36.
- [49] Faghieh R, Dwight W, Pan JB, Fox GB, Krueger KM, Esbenshade TA, et al.  $\alpha$ -Alanine piperazine-amides: novel non-imidazole antagonists of the histamine  $H_3$  receptor. *Bioorg Med Chem Lett* 2003;13:1325–8.
- [50] Dvorak CA, Apodaca R, Barbier AJ, Berridge CW, Wilson SJ, Boggs JD, et al. 4-Phenoxypiperidines: potent, conformationally restricted, non-imidazole histamine  $H_3$  antagonists. *J Med Chem* 2005;48:2229–38.
- [51] Morini G, Comini M, Rivara M, Rivara S, Lorenzi S, Bordini F, et al. Dibasic non-imidazole histamine  $H_3$  receptor antagonists with a rigid biphenyl scaffold. *Bioorg Med Chem Lett* 2006;16:4063–7.
- [52] Sasho S, Seishi T, Kawamura M, Hirose R, Toki S, Shimada JI. Diamine derivatives containing imidazolidinylidene propanedinitrile as a new class of histamine  $H_3$  receptor antagonists. *Part I. Bioorg Med Chem Lett* 2008;18:2288–91.
- [53] Lau JF, Jeppesen CB, Rimvall K, Hohlweg R. Ureas with histamine  $H_3$ -antagonist receptor activity—a new scaffold discovered by lead-hopping from cinnamic acid amides. *Bioorg Med Chem Lett* 2006;16:5303–8.
- [54] Jitsuka M, Tsukahara D, Ito S, Tanaka T, Takenaga N, Tokita S, et al. Synthesis and evaluation of a spiro-isobenzofuranone class of histamine  $H_3$  receptor inverse agonists. *Bioorg Med Chem Lett* 2008;18:5101–6.
- [55] Cumming P, Vincent SR. Inhibition of histamine- $N$ -methyltransferase (HNMT) by fragments of 9-amino-1,2,3,4-tetrahydroacridine (tacrine) and by  $\alpha$ -Carboline. *Biochem Pharmacol* 1992;44:989–92.
- [56] Schlegel B, Laggner C, Meier R, Langer T, Schnell D, Seifert R, et al. Generation of a homology model of the human histamine  $H_3$  receptor for ligand docking and pharmacophore-based screening. *J Comp Aided Mol Des* 2007;21:437–53.
- [57] Labeuw O, Levoine N, Poupardin-Olivier O, Calmels T, Ligneau X, Berrebi-Bertrand I, et al. Novel and highly potent histamine  $H_3$  receptor ligands. Part 2: Exploring the cyclohexylamine-based series. *Bioorg Med Chem Lett* 2011;21:5384–8.
- [58] Levoine N, Labeuw O, Calmels T, Poupardin-Olivier O, Berrebi-Bertrand I, Lecomte JM, et al. Novel and highly potent histamine  $H_3$  receptor ligands. Part 1: Withdrawing of hERG activity. *Bioorg Med Chem Lett* 2011;21:5378–83.
- [59] Barbier AJ, Berridge C, Dugovic C, Laposky AD, Wilson SJ, Boggs J, et al. Acute wake-promoting actions of JNJ-5207852, a novel, diamine-based  $H_3$  antagonist. *Br J Pharmacol* 2004;143:649–61.
- [60] Cowart M, Pratt JK, Stewart AO, Bennani YL, Esbenshade TA, Hancock AA. A new class of potent non-imidazole  $H_3$  antagonists: 2-aminoethylbenzofurans. *Bioorg Med Chem Lett* 2004;14:689–93.
- [61] Horton JR, Sawada K, Nishibori M, Cheng X. Structural basis for inhibition of histamine  $N$ -methyltransferase by diverse drugs. *J Mol Biol* 2005;353:334–44.
- [62] Hancock AA. The challenge of drug discovery of a GPCR target: analysis of preclinical pharmacology of histamine  $H_3$  antagonists/inverse agonists. *Biochem Pharmacol* 2006;71:1103–13.

- [62] Apodaca R, Dvorak CA, Xiao W, Barbier AJ, Boggs JD, Wilson SJ, et al. A new class of diamine-based human histamine H<sub>3</sub> receptor antagonists: 4-(aminoalkoxy)benzylamines. *J Med Chem* 2003;46:3938–44.
- [63] Simulations Plus, Inc.. ADMET predictor v. 6.5. 42505 10th Street West, Lancaster, CA 93534-7059 USA: Simulations Plus, Inc.; 2013(<http://www.simulations-plus.com/>).
- [64] Advanced Chemistry Development, Inc.. ACD/i-Lab freeware. Toronto, ON, Canada: Advanced Chemistry Development, Inc.; 2012, ([www.acdlabs.com/](http://www.acdlabs.com/)).
- [65] Bembenek SD, Keith JM, Letavic MA, Apodaca RD, Barbier AJ, Dvorak L, et al. Lead identification of acetylcholinesterase inhibitors-histamineH<sub>3</sub> receptor antagonists from molecular modeling. *Bioorg Med Chem* 2008;16:2968–73.
- [66] Morini G, Comini M, Rivara M, Rivara S, Bordini F, Plazzi PV, et al. Synthesis and structure–activity relationships for biphenyl H<sub>3</sub> receptor antagonists with moderate anti-cholinesterase activity. *Bioorg Med Chem* 2008;16:9911–24.
- [67] Darras FH, Pockes S, Huang G, Wehle S, Strasser A, Wittmann HJ, et al. Synthesis, biological evaluation, and computational studies of tri- and tetracyclic nitrogen-bridgehead compounds as potent dual-acting AChE inhibitors and hH<sub>3</sub> receptor antagonists. *ACS Chem Neurosci* 2014;5:225–42.